MANGO Classes-Modelica Classes of the Norvegian Grid for iTesla and Software-to-Software Validation

August 18, 2014

MENGJIA ZHANG

KTH Electrical Engineering

Master's Degree Project
Stockholm, Sweden 2014

XR-EE-EPS 2014:009

School of Electrical Engineering, KTH Royal Institute of Technology, Sweden

Electrical Power Systems Division

MANGO Classes-Modelica Classes of the Norvegian Grid

for iTesla and Software-to-Software Validation

— Diploma Thesis —

Supervisor:
Maxime Baudette

Examiner
Dr. Luigi Vanfretti

February 2014 to August 2014

Abstract

Recent efforts of collaboration between the European transmission system operators have led to an increased interest in common research projects concerning power system analysis. The iTesla project is an example of European collaboration that focus on developing common tools for the simulation and analysis of large scale power systems. The work carried out during the thesis is a part of the iTesla project in which Modelica has been selected as a common simulation platform. The work encompasses the development of Modelica classes for power grid components used in different Norwegian grid dynamic Models.

The simulation platform PSS/E is used as a reference software for the developed power system models. In this thesis power system models have been implemented in Modelica. The performance of these Modelica classes have been validated through comparing between the behavior of the developed and reference models in dynamic simulations. The validation process simulating several small scale power system models and a subset of the Norwegian grid model that have been identically implemented in both simulation platforms. The results from the dynamic simulation under different perturbation have been compared in accuracy to validate the work.

Acknowledgments

There are a lot of people I would like to thank for help me during this thesis work. Firstly, I'd like to thank my supervisor and examiner Prof. Luigi Vanfretti for giving me the opportunity to carry out a small project to build Modelica SVC models last summer and then further providing me the chance to work on this project. I'd like thank him also for trusting me and providing me with the necessary training about Modelica and PSS/E in order to carry out this thesis's work. Further more, I'd like to thank him for being patient with me, providing guidance generously, and encouraging me to explore and carry out my own idea during working.

Secondly, I'd like to thank my direct supervisor Maxime Baudette for keeping good track and providing good advices for my work. His suggestions towards the my report and presentation of the project are really appreciate.

Finally, I'd like to thank Statnett for their help in the project by providing information and resources of the power grid models. Also I'd like to thank my colleagues in SmarTS Lab group at EPS (Electrical Power System)department of KTH (The Royal Institute of Sweden)for having good discussion with me which helps me to organize my analysis. Also I would like to thank my parents and all of my friends. Thank them for providing good accompany encouragement.

Mengjia Zhang
June

Contents

Notation **ix**

1 Introduction **1**
1.1 Background . . . 1
1.2 iTesla . . . 1
1.3 Objectives . . . 2
1.4 The outline of the thesis . . . 2

2 Software Environment **3**
2.1 Introduction to PSS/E . . . 3
2.1.1 Power System Models and Simulation Procedure . . . 3
2.1.2 Integration Algorithm . . . 4
2.2 Introduction to Modelica . . . 5
2.2.1 Modelica Langange Specification . . . 5
2.3 Dymola, the Modelica simulation environment . . . 7
2.3.1 solvers . . . 9

3 Model Development and Implementation **11**
3.1 Electrical Components . . . 12
3.1.1 Basic Composite Load . . . 12
3.1.2 Frequency dependent load . . . 14
3.1.3 Transformer Models . . . 15
3.1.4 Synchronous generator . . . 20
3.2 Nonelectrical Element . . . 24
3.2.1 Excitation System . . . 24
3.2.2 Power System Stabilizer . . . 30
3.2.3 Governor System . . . 32

4 Model Validation **37**
4.1 Small-Scale Power System Tests . . . 38
4.1.1 Validation of Genrou . . . 42
4.1.2 Validation of Gensal . . . 45
4.1.3 Validation of IEEET2 and IEESGO . . . 47
4.1.4 Validation of SCRXS and HYGOV . . . 50
4.1.5 Validation of IEEET1, STAB2A and LFDRAL . . . 51
4.1.6 Validation of OLTC . . . 56
4.2 Real World Power System . . . 58
4.3 AKD . . . 58
4.3.1 System Setup . . . 58
4.3.2 Validation result . . . 58

5 Conclusion **61**

A Appendix **63**
A.1 Dynamic parameter 63

Notation

$\Delta\omega$	per unit speed deviation from synchronous
δ	angle between quadrature axis and terminal voltage
ω	per unit speed of generator
ψ'_d	direct axis flux linkages
ψ'_q	quadrature axis flux linkages
E'_d	Voltage proportional to quadrature axis flux linkages
E'_q	Voltage proportional to direct axis flux linkages
e_d, e_q	Armature voltage, direct and quadrature axis components
E_{fd}	generator field voltage(one per unit is the value for 1 per unit terminal voltage on the air gap line, open circuit)
i_d, i_q	Armature current, direct and quadrature axis components
P	active power
P_e	electrical power
Q	reactive power
T_e	electrical torque
T_m	mechanical torque
v_t	terminal voltage
$x(t)$,x	vector of differential variables
$y(t)$,y	vector of differential variables
BDF	Backward Differentiation formula
DAE	Differential and Algebraic Equations
ODE	Ordinary Differential Equations
PSAT	Power System Analysis Toolbox
PSS/E	Power System Analysis for Engineer
SMIB	Single Machine Infinite Bus
SPS	SimPowerSystem

1 Introduction

1.1 Background

Over the past decades the European electricity networks have changed drastically. The environmental impact of the energy production has become a major driver of the extension of the European grids. Thus, the share of renewable energy sources is increasing, bringing always more intermittent energy sources. Also, the progressive construction of a single European electricity market leads to more power exchanges across Europe. As a results the Pan-European electricity networks are becoming more and more complex to be operated. This has led to an increased need of collaboration between the different European transmission system operators (TSOs), which in turn motivated more common research projects in the power system domain.

The harmonization of this domain is indeed a key factor for the success of the operation of the future grid. However, nowadays, most TSOs use different simulation software for carrying out system analyses. This fact introduces the obstacle on the way towards harmonizing operation procedure since models and data format can not be transferred easily from one software to another. Numerous efforts have been made by power system community on facilitating the model exchange between different simulation platforms. But all the dynamical aspect of the modes is left apart for now.

1.2 iTesla

The Innovation Tools for Electrical System Security within Large Area, iTesla project[1], is an example of such research collaboration between European institutes and TSOs. The goal of the project is to develop and validate an open inter-operable toolbox which will be able to support the future operation of the Pan-European grid[1]. One of the challenge which the tool box has to take up is to perform accurate security assessments taking into account the dynamics of the system using time-domain simulations. This will be achieved through the development of different tolls and algorithms that will be validated with reference power system network models. This work requires, however, a simulation platform for power system models that is both common among the participants of the project, and extensible enough for being used by the tools to be developed.

In the contexts of this project, the Modelica language was selected to be the common simulation environment. The different models for power system networks will be developed in Modelica language, which will require the development of all the power system components as dynamic models. All of the models developed will contribute to creating a library. Modelica, as a multi-domain, equation base, declarative programming language, satisfies all the requirements for modeling complex power system with such consistent format of dynamic power grid models. By utilizing equations, the causality of the models are eliminated and by adopting the declarative programming method, the modeling and simulation algorithm are completely separated [14]. Thanks to these features of Modelica, the work of modelers remain only deriving mathematical representation of

the models instead of building the equations as well as designing the computation procedure of the them. Also, Modelica language is very easy for one to understand which will facilitate the reuse of modeling knowledge and speed up the procedure of building new models and verification the old ones.

Currently, Modelica community continues making more effort on releasing Modelica as a standard language. As it is a standardized language, model exchange will never be a problem as long as every modeler build models according to Modelica specification. There are now several simulation platforms which can support Modelica language both commercially and free of charge. Such as OpenModelica, JModelica, Dymola, MapleSim, SimulationX, Mathematica, SystemModeler etc. The Modelica code can also be exported and be simulated in other software which is widely used in today's industry such as MATLAB thanks to the function of Flexible Mock-up Interface (FMI). This feature enables future optimization and the on-line identification of power system models.

1.3 Objectives

This thesis was carried out as a collaboration with the Norwegian grid, Statnett, as part of their involvement in the iTesla project. Statnett will provide some of the reference models for iTesla. These models were correctly developed in the PSS/E software and will need to be implemented in the Modelica language. The work was divided into two projects: MANGO classes, whcih if focusing on the development of Modelica classes for each component model used in the Norwegian grid models; and MANGO models, which is focusing on the development of the grid models in Modelica. The work presented here is related to the first projects.

The work in this thesis is further divided into two parts: implementation and validation. There are two problems should be solved during the stage of implementation. The first one is to derive the correct mathematical representation of the models and the second one is to solve the initialization problem of them. Once all of the models are ready, different simulation tests should be performed in order to validate the performance of the developed models. The procedure contains four steps: building small scale power system models in reference software PSS/E, finding proper scenario and recording simulation results, setting up the same test systems in Dymoal and finally comparing the performance from two software.

1.4 The outline of the thesis

The remaining parts of the thesis is organized as follows. Firstly, a brief introduction of the software PSS/E and the specification of Modelica language are given in Chapter 2. Chapter 3 covers the mathematic representation of the dynamic Norwegian grid components. After that, the readers are supposed to have the basic idea of how the implementation should be performed. Chapter 4 describes some examples to further explain the detail of implementation method of the components. The results of validation are analyzed in Chapter 5. The discussion based on the validation results will be presented in Chapter 6. The thesis is ended by the conclusion and future work in Chapter 7.

2 Software Environment

This chapter gives a brief introduction to the main software environments used in this thesis. As explained in the introduction, the work will utilize two different software environments, namely Power System Simulator for Engineer (PSS/E) and Modelica. The first part of this Chapter provides a brief introduction of PSS/E including a general explanation of the network modeling method, the simulation engine algorithm and the dynamic analysis procedure of the software. Secondly, the Modelica language together with Dymola will be introduced. A brief explanation of the layout and basic function of Dymola and a brief summary of the key specification of the Modelica language will be provided.

2.1 Introduction to PSS/E

PSS/E is an integrated set of computer programs for studies of power system transmission network and generation performance in both steady-state and dynamic conditions. Considering timescale, PSS/E focuses on the analysis of electromechanical transient behavior of the generators and their controls named transient stability analysis.

2.1.1 Power System Models and Simulation Procedure

Power systems in PSS/E are modeled by a set of algebraic equations for the voltages and currents phasors at the fundamental frequency. The dynamic behavior of the system depends on the differential equations of the flux linkage, rotor speed, and controllers of generators. The transmission system of the network is modeled by linear algebraic equations of the voltage and current phasors derived from Kirchhoff's laws. The nonlinearity is introduced by the characteristics of generators and loads such as the magnetic saturation function of generators. The interface between the electrical components and the network uses the specific voltage-current characteristics determined by each dynamic components.

The software PSS/E has several power flow routines, where the equations of the network are expressed as constant admittance matrix. Both transmission lines and transformers are modeled by equivalent series and shunt admittance, but the difference is that a complex nominal tap ratio introduced by transformers can allow modification of voltage phasors at both ends. During dynamic simulation, however, the dynamic of the generators and the loads demands are included, which requires a conversion step. The synchronous generators are modeled by a Norton equivalent of which the instantaneous values are governed by the differential equations of rotor speed and flux linkages. Loads are modeled as a adjustable mix of constant current characteristic and constant impedance characteristic. After conversion of loads and generators, the admittance matrix is updated and the power flow solution is update for compensating the small mismatches introduced by the conversion step.

The dynamic simulation begin by an initialization step using the power flow data. The internal initialization of every components is performed using the algebraic equations of the models and the new set of equations derived from the differential equations of the models by setting the time derivate of the state variables to be zero. Thus the dynamic simulation starts from a point of steady state operation.

The main skeleton of PSS/E only contains logic for data input, output, numerical integration, and electric network solution, but contains no logic related to differential equations of dynamic equipments. They are written in subroutines. Whenever there are needs to calculate the numerical values of time derivatives for one dynamic equipment, the corresponding subroutine which contains such calculation logic is then called by the main skeleton for initialization stage or for dynamic simulation within each time step. The procedure is shown as in Fig 2.1.

PSS/E allows user-defined models, but the development procedure is rather complicated. It

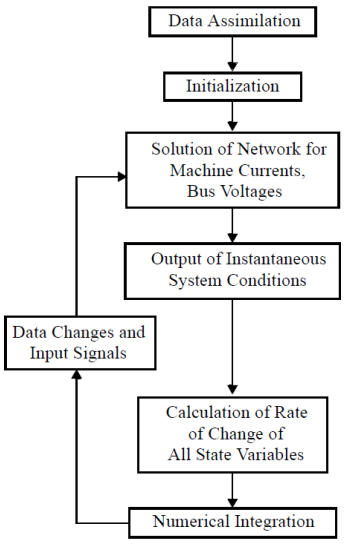
Data Assimilation
Initialization
Solution of Network for Machine Currents, Bus Voltages
Output of Instantaneous System Conditions
Data Changes and Input Signals
Calculation of Rate of Change of All State Variables
Numerical Integration

Figure 2.1: PSS/E simulation procedure[9].

implies to identify the different state variables of the model and derive the equations for their integration. The model should also include the interfacing code defining the causality of the system as well as handling the data input. However, all models are to be developed in FORTRAN or FLECS and compiled for their integration into PSS/E preventing any future editing.

2.1.2 Integration Algorithm

The integration technique applied in PSS/E is an explicit method belonging to the family of the Second-Order Runge-Kutta method[9]. PSS/E solver applies integration algorithm to the values taken from the last iteration to calculate the new values. The nature of this computation process is discrete and can be viewed as a transfer function. Thus, it was expressed in a Z-transform form shown below.

$$F(Z) = \frac{h(3Z-1)}{2Z(Z-1)}$$

Applying the inverse Z-transform leads to the time domain equation which yields a Two-step Adams-Bashforth method shown here.

$$x_k = x_{k-1} + \frac{h}{2}(3f_{k-1} - f_{k-2})$$

2.2 Introduction to Modelica

Modelica is an equation-based object-oriented modeling language which is capable to describe both continuous and discrete dynamics of physical systems in a convenient way by a set of differential, algebraic and discrete equations. Modelica enables the acausal equation-based description of the complete physical systems by a set of interconnected multi-domain subsystems, which include the dynamic description with a set of mathematical equations, and the interconnection equations[14]. The language is built by an independent association, the Modelica Association [2], who releases the specifications. The specifications give the details of the supported functions, the syntax and the dedicated syntax for graphical representation of the model.

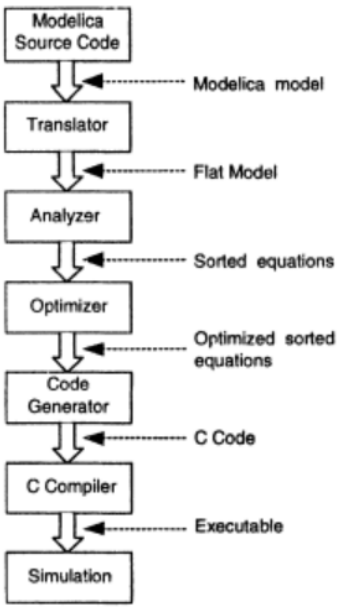

Figure 2.2: Translation stages from Modelica code to executing simulation[12]

2.2.1 Modelica Langange Specification

The modelica language is an object-oriented language. Thus, any model is built as a class with a set of attributes and a set of equations. The following sections will present the fundamentals of the language.

2.2.1.1 Class/ Attributes

The Modelica languages defines a set of build-in classes and types that can be used as attributes in addition to all the other user-defined classes. The attributes of a Modelica class contains: constants, parameters, and variables. By default, all of the variables are continuous time variables which might evolves their values continuously during simulation. The specific *time variability* for variables can be declared by prefixes *constant, parameter, discrete*. Constants will never change their value once they have been defined,$e.g.$,$\pi = 3.1415926$..... The value of the variables declared as *parameter* can be assigned by users before simulation or after the stage of initialization, but will remain constant during time-dependent simulation. The *discrete* variables can change their values only at event instants during simulation. Furthermore, *time* is a global built-in variable, which can be used without declaration.[13]. There are four types of variable by default which are

shown in Table 2.1:

Table 2.1: Available default variable types

Types	Description
Real	floating point,$e.g.1.0, -2.3e-5$
Integer	integer,$e.g.1, -4, 333$
Boolean	boolean,$e.g.$ false, true
String	string, $e.g.$ "from file:"

For the sake of making the code more readable and easier to maintain, special keywords as shown in Table 2.2 are utilized to describe specific class[13].

Table 2.2: Modelica Classes Overview

Types	Description
type	Class to define variable types
connector	Class to define interfaces
model	Class to define model components
block	Like model class, but only public input, output or parameter
function	no internal states, with algorithm section and function-call syntax
package	Class to define library, no equations
record	Class to group variable declarations, no equations

2.2.1.2 Equations/ Algorithm

Equations are added in the equation section after the **equation** keyword. Differential equations are expressed with the **der**-operator. It denotes the time derivative of the expression following in brackets, the state variable. The states are integrated by the numerical solver to find the solution ot the problem. Each state requires an initial condition. As the solver will proceed to a symbolic manipulation of the equation set, there is no requirement on their order nor on their form (e.g. $a + bx = x'$ is equivalent to $x' - a = bx$). Each component must have a set of equations that uniquely define its behavior based on its interfaces and initial conditions. There are the following types of equations:

Table 2.3: Equation Types

Type	Example
initial equation	der(w)=0
Equality equation	$V = R \times I$
Connection equation	**connect**(pwpin1.n,pwpin2.p)
Conditional equation	if-then; when-end when

Connectors are special types of Modelica classes defining an interface to a model which rules the physical properties at the boundaries of the models. A connection between two connectors will generate equations based on two types of connection rules: equality and sum-to-zero. For all connector variables declared with prefix **flow**, only one equation will be generated per connection set $i.e. i_1 + i_2 + i_3 = 0$. Those without prefix by default is set to be potential variables, and $n - 1$ equations based on equality rule will be generated per set. Connection between connectors are regards as equations. The direction of data flow in the connection is treated without causality. But when the flow directs towards inside of the component, the sign of the variables are considered as

positive by convention. Additionally, one can also specify causal connection by declaring connector as *input* or *output*.

2.2.1.3 Modelica libraries

Modelica like any other object-oriented language is built to reuse existing code. Thus, any collection of models can be gathered as package that are commonly referred to as libraries. These can be imported in the modeling environment and used in the models being developed. In this work, two libraries were mainly used, namely, the Modelica Standard Library and the PowerSystem library.

Modelica standard library

The Modelica standard library (MSL) is a free library developed by Modelica Association. The overview of the library is shown in the left side of Fig. 2.3. The elements in the library can be used to model multi-domain systems including mechanical (1D/3D), electrical (analog, digital, machines), thermal, fluid, control systems and hierarchical state machines. To build a system, one can drag-and-drop the components from the library to the graphical edit screen. Also numerical functions and functions for strings, files and streams are included[2]. This thesis utilize several basic blocks such as transfer functions and some numerical functions to build the component models for control and protection systems.

PowerSystems library

The PowerSystems library is developed within *iTesla* project shown in Fig. 2.3. The elements in the library can support phasor time-domain simulation of power system models. The dynamic components models developed in this thesis project will finally be integrated into this library. Some of the simple models such as **Pwline** and **Pwpin** are utilized in this thesis. **Pwline** is a pi-equivalent model of transmission line. And **Pwpin** is the connector for setting up connection between electrical components.

PwPin defines voltage and current as complex variables. Four variables are declared within **PwPin** connector, and they are real and imaginary part of potential variables voltage and flow variables current. For other components like synchronous machines regulator, **Realinput** from Modelica library are adopted, and only potential variables are declared for signal communication.

2.3 Dymola, the Modelica simulation environment

As the Modelica is developed as a language with detailed specification, several tolls have been developed by different vendors to support it. The development and simulation environment used in this work is Dymola, the Dynamic Modeling Laboratory, from Dynasim company[3]. Dymola incorporates a set of advanced solvers that can perform simulations of complex hybrid systems.

The tool's interface is divided into two tabs, one dedicated to the models development, and the other dedicated to the simulations. The modeling environment is shown in Fig. 2.4. In this mode, models can be explored, edited or created. It features a package browser for drag-and-drop interactions for building more complex models from single blocks.
The simulation model is activated when clicking on the simulation tab in the Power-right corner of the interface. Thus, the interface switches to an environment for carrying out simulations and analyzing of the results, as depicted on Fig. 2.5. The first step is the syntax check, that will ensure that the model is correct regarding the syntax itself, the balance in number of variables and equations and the number of initialization equations. The next step is the simulation that will perform all the steps of equation set analysis, simplification, flattening and compilation to

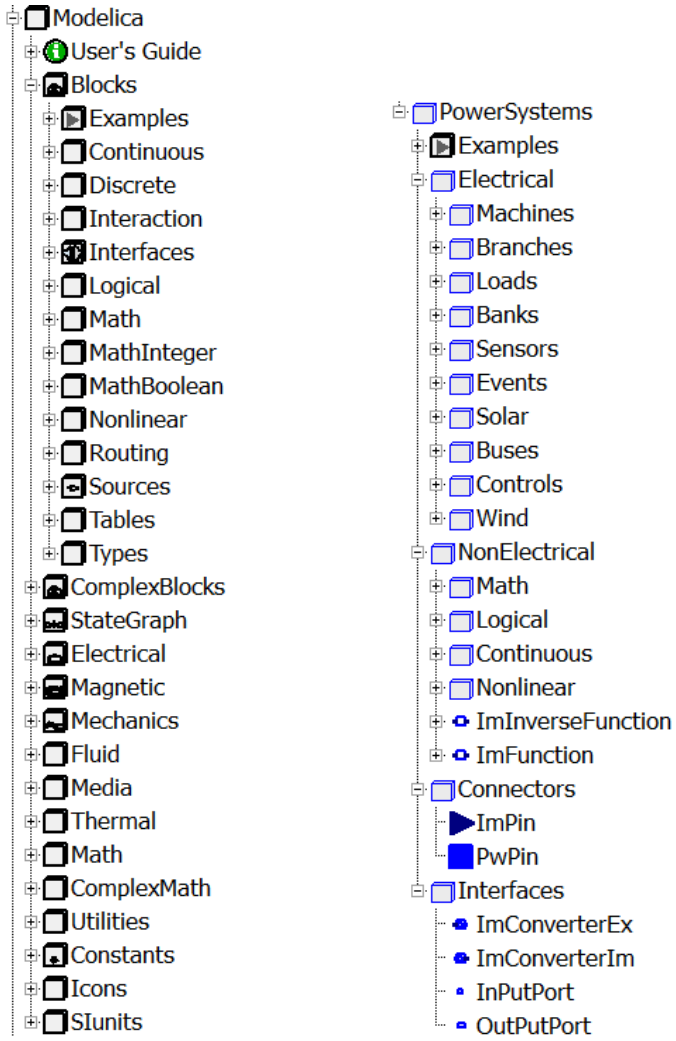

(a) Modelica standard library.

(b) PowerSystems Library.

Figure 2.3: Overview of MSL and PowerSystems Library.

executable C-code before starting the simulation.

The information about these intermediary steps can be shown in the translation log, with for example, the number of linear and non-linear equations. Note that the simulation settings can be configured in this interface through a configuration dialog shown on Fig. 2.6. The default settings use the DASSL solver with a tolerance of 0.0001 and retain 500 intervals to plot.

After performing the simulation, the variables are accessible through variable browser which contains parameters and variables of the simulated model. Except those defined with prefix **protected**, all of the variables will be listed hierarchal in the browser and can be plotted by drag-and-drop the variables to the plot diagram. Up to 99 different simulation results can be shown simultaneously in the Variable Browser. Furthermore, the information about the executed simulations such as CPU time, function and Jacobian evaluations, and the number of events and result points are available in the prompt up simulation log.

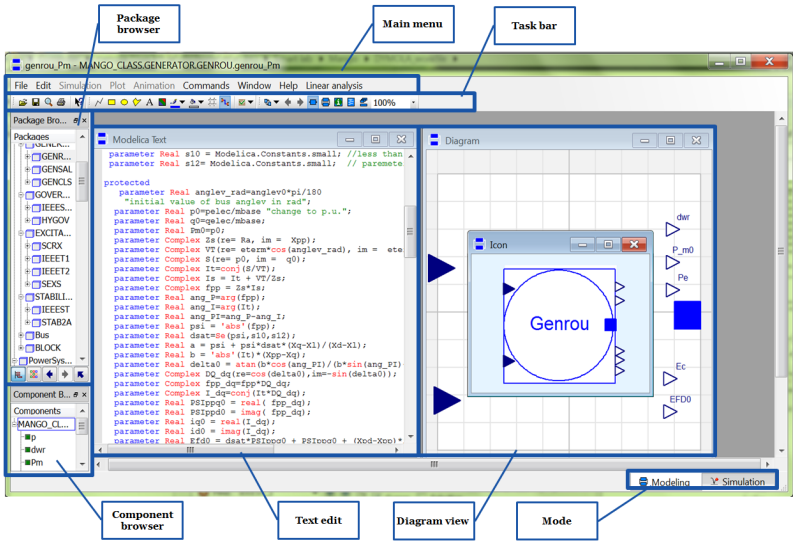

Figure 2.4: Screen shot of the Interface of Dymola (Modeling mode)

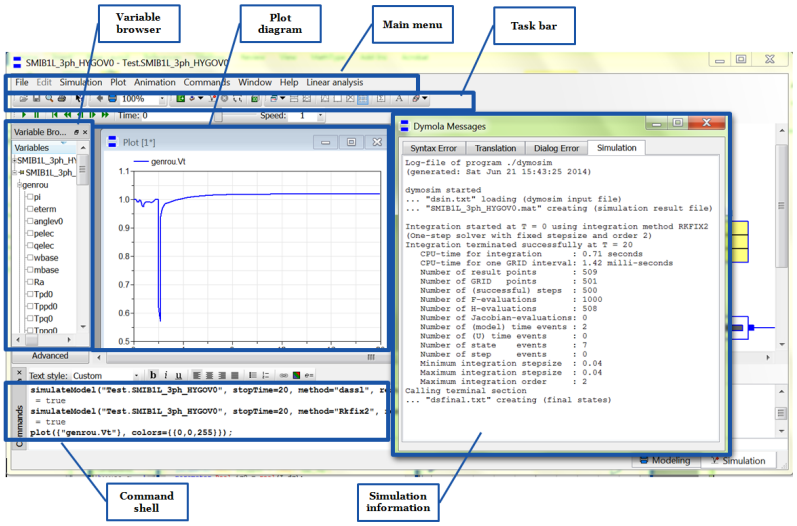

Figure 2.5: Screen shot of the Interface of Dymola (Simulation mode)

2.3.1 solvers

Currently, Dymola provides ten different integration methods with fixed step size and variable step size. An integration method approximates the solution internally by a polynomial of order k. Some methods such as Euler, Rkfix use a fixed order while other methods such as DASSL, LSODAR vary the order during simulation. In this work, only the Rkfix 2 and DASSL integration method were used.

Rkfix2 is a 2^{nd} order Runge-kutta fixed step solver. This method can only handle the ordinary differential equation type, no stiff system models. Although power system models contain DAEs, Dymola converts the model to explicit ODE form first before the simulation. All of the tests in this thesis project have used Rkfix2 as solver since this is the most similar one to the PSS/E solver. The equation of the algorithm is shown as below.

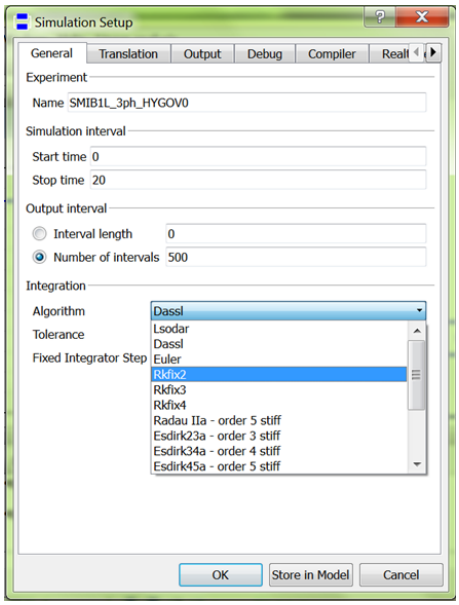

Figure 2.6: Over view of Dymola

$$x_{k+1} = x_k + hf(t_k + \frac{1}{2}h, x_k + \frac{1}{2}hf(t_k, x_k))$$

DASSL is a variable-step, variable-order method which implements the backward differentiation formula (BDF) from order one to five in DAE format. Since the integration method used by the DASSL solver differ strongly from the one used by PSS/E. It will only by used during development phases in this thesis.

3 Model Development and Implementation

The goal of the this thesis is to build a corresponding Modelica class for each component model used in the Norwegian grid. There are seventeen models in total was developed in this project. The models include synchronous machines and its regulators, transformers and composite load models. The detail of modeling method was described in this chapter.

The models were originally developed in PSS/E. Thus it is necessary to fully study the documentations of PSS/E to first understand the modeling background and usage of each component model and then implement the model in Modelica language srespect to the model specification.To implement the model in Modelica, it is suggested that one should follow the following two steps:

1. **Define the input/output interface of the model.** The power grid components will finally be connected and integrate to different system models. Each components take information from system and influence the system's behavior by varying its output respect to its own dynamics. There are two different types of interface are available for power system modeling: electrical connector and nonelectrical connector. Electrical connector is a special type of Modelica class which contains four variables to represent the voltage and current phasor. The power flow information is transferred from one electrical connector to another. Nonelectrical connectors are mainly real input/output connectors which are utilized to connect different blocks of control system.

2. **Declare the attributions of each model.** The parameters and input/output variables should be declared respect to the model specification. The equations of could be declared as normal equations or connection equations which depends on the modeling method of the models. In this these, all electrical components were modeled textually where normal equations were utilized while nonelectrical components were modeled graphically where connection equations were applied.

3. **Solve the initialization problem of the model.** A start value should be provided for each state variable in order to give a start point for the integrator of the software to process calculation. The whole start value set are called the equilibrium of the system. Generally, the equilibrium are calculated by power flow which omits the detailed dynamics of the devices. Thus extra calculation should be performed within the model to obtain the initial value of each state.

The rest of this chapter will go through the modeling procedures of all the models. The models are characterized into two categories: electrical components and nonelectrical components. Electrical components are models which participate in power flow directly such as synchronous machines, transformers, composite loads, and static-var-compensator. Nonelectrical components are models which are signal process systems working to control the system such as excitation system, governor system, stabilization system and on-load-tap-changer.

3.1 Electrical Components

3.1.1 Basic Composite Load

The composite load model from PSS/E includes a load conversation procedure and special dynamic variation function. Although there are already load models in the PowerSystem library, none of them was matching the load mode available in PSS/E. Since the load model plays a crucial role in power exchange, it is necessary to implement the same load model in order to have the same test system in both software. The focus are first implement the model to represent the mentioned special feature of the composite loadd in PSS/E and then further developed the model to include the frequency dependent characteristic and the function of load varying.

The PSS/E load model is defined by a constant MVA load for steady-state studies. The value is then converted for the dynamic studies into a mix of constant power, constant current, and constant admittance load components with user defined portion ratio. After that the resulted constant current and constant admittance load is added to any existing load represented by those characteristics.

The converting process following the rules below:

$$\begin{aligned} S_I &= S_i + \frac{aS_p}{V} \\ S_Y &= S_y + \frac{bS_p}{V^2} \\ S_P &= S_p \times (1 - a - b) \end{aligned} \tag{3.1}$$

where:

S_p	Original constant MVA load
S_i	Original constant current load
S_y	Original constant shunt admittance load
S_P	Final constant MVA load
S_I	Final constant current load
S_Y	Final constant shunt admittance load
a, b	Load transfer fractions,$(a + b) < 1$
V	Magnitude of bus voltage when load conversion is made

The PSS/E models also include a shedding factor for the constant power load share when the voltage level goes under a predetermined threshold. This threshold is set in the solution parameter **PQBRAK**. The resulting characteristic is shown in Fig. 3.1(a) which describes the behavior of the constant power load as functions of bus voltage respecting to different **PQBRAK** with values of $0.6, 0.7, 0.8$ p.u.. Similarly, the amount for constant current load share should be reduced when the bus voltage goes below 0.5 p.u. as shown in Fig. 3.1(b). These feature are represented by a shedding factor that is multiplied to the normal values.

Even thought the PSS/E documentation provides the figures 3.1(a)and 3.1(b), the exact equations of these curves is not documented. The figures were therefore used in MATLAB to find the best fitting expressions that will be used for the Modelica models. In this thesis, only two curves are extracted, one is the shedding factor function $K_P = f(V)$ for constant power load with **PQBRAK** of 0.7, the other is that of constant current load, $K_I = f(V)$.

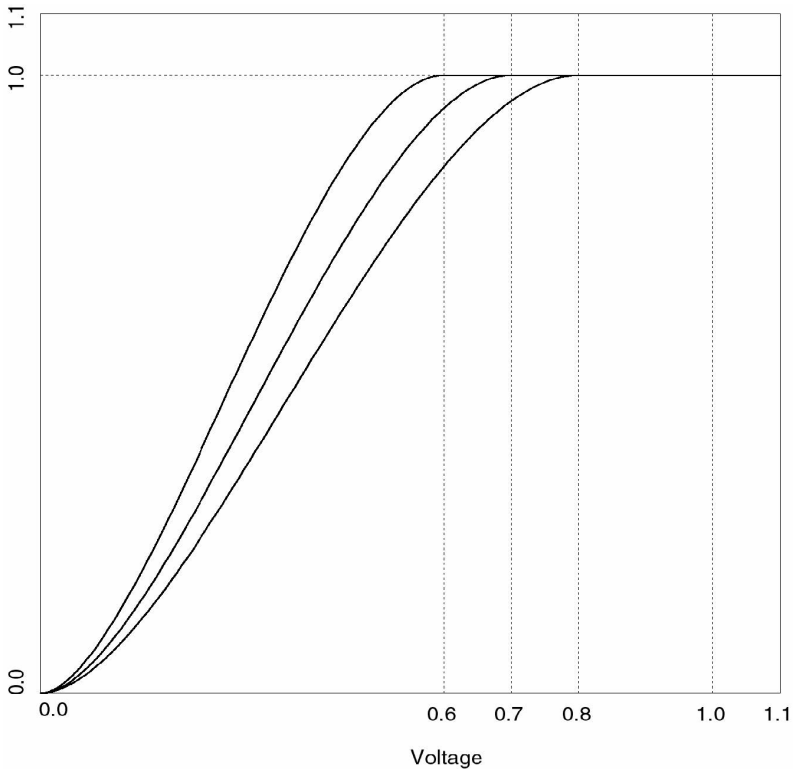

(a) Constant Power Load Characteristic

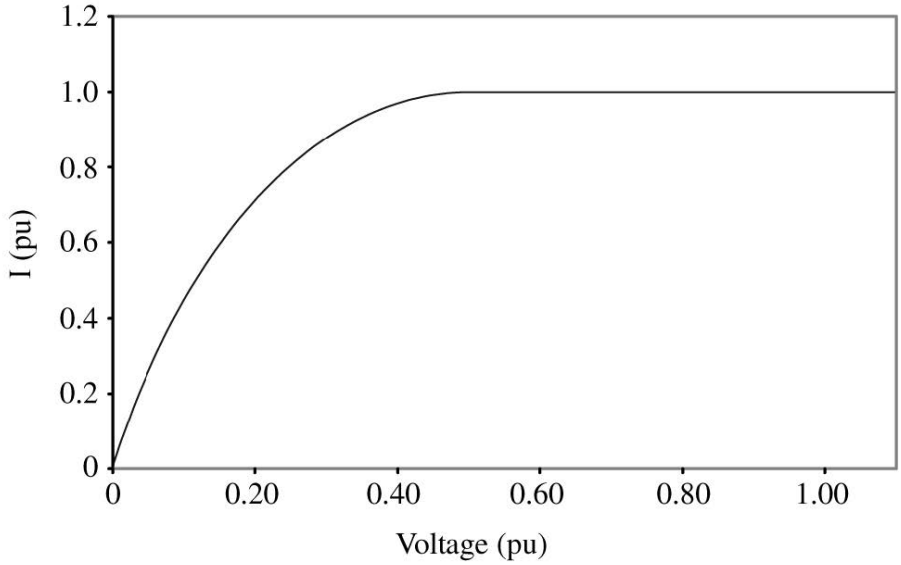

(b) Constant Current Load Characteristic

Figure 3.1: PSS/E Specified Load Characteristic

$$K_P = \begin{cases} 0.4881 - 0.4999\cos(3.964V) + 0.1389\sin(3.964V) & V < 0.7 \\ 1 & V \geqslant 0.7 \end{cases} \tag{3.2}$$

$$K_I = \begin{cases} 2.657V^{0.769}\exp\left(-1.502V^{1.769}\right) & V < 0.5 \\ 1 & V \geqslant 0.5 \end{cases} \tag{3.3}$$

The model developed in Modelica for a composite load adopts the same strategy as the PSS/E model, but includes also all the function related to the conversion and saturation. Therefore, the user is offered the possibility to configure the following parameters shown in Table 3.1:

Table 3.1: Composite Load Parameters

Parameter	Type	Description	Unit
S_p	Comp.	Original constant power load	p.u
S_i	Comp.	Original constant current load	p.u
S_y	Comp.	Original constant shunt admittance load	p.u
a	Comp.	Coverting fraction for constant I load	-
b	Comp.	Coverting fraction for constant Z load	-
PQ_{BRAK}	Real	Constant power characteristic threshold	p.u.

The voltage and current characteristics for the load should be then specified as following:

$$\begin{aligned} &P + jQ = \vec{V}\vec{I} \\ &P = K_P\Re(S_P) + K_I\Re(S_I)V + \Re(S_Y)V^2 \\ &Q = K_I\Im(S_P) + K_I\Im(S_I)V + \Im(S_Y)V^2 \end{aligned} \tag{3.4}$$

3.1.2 Frequency dependent load

In addition to the composite load model presented previously, the Norwegian grid model includes a frequency dependent model. The model used in PSS/E is LDFRAL. The model makes the constant current and MVA components of all loads dependent on bus frequency according to following rules:

$$\begin{aligned} P &= P_o(\frac{\omega}{\omega_o})^m \\ Q &= Q_o(\frac{\omega}{\omega_o})^n \\ I_p &= I_{po}(\frac{\omega}{\omega_o})^r \\ I_q &= I_{qo}(\frac{\omega}{\omega_o})^s \end{aligned} \tag{3.5}$$

where the frequency is derived from the derivative of the load bus angle. *wbase* in the equation is the base frequency.

$$\dot{Angle} = wbase \times \omega$$

In the above equations, P, Q, I_p, I_q stand for the value of the load respect to constant power and constant characteristic respectively. The power share of the load depends on the original value multiplies the power of nominal frequency with user defined power factor for different load share. Thus for LDFRAL, there are four additional parameter need to be configured.

Table 3.2: Frequency Dependent Composite Load Parameters

Parameter	Type	Description	Unit
m	Real	Real power load frequency exponent	-
n	Real	Reactive power load frequency exponent	-
r	Real	Real current load frequency exponent	-
s	Real	Reactive current load frequency exponent	-

3.1.3 Transformer Models

In this section two transformer models will be presented; a two-winding transformer model and a three-winding transformer model. Both models are capable to include a phase shift function and an on load tap changer (OLTC) function. The detail of derivation procedure of the per-unit transformer equivalent circuit will not be covered, for further information, one can refer to [6][9].

3.1.3.1 Two Windings Transformer

The standard PSS/E two-winding transformer represent the equivalent one line diagram shown in Fig. 3.2. This is the standard positive sequence transformer model as recognized by the great majority of utility databases and by the IEEE Common Format for Exchange of Solved Load Flow Cases. The quantities from the primary side are indicated with the subscript "i" and the quantities from the secondary side with the subscript "j". Users can specify the per-unit equivalent resistance R and reactant X.

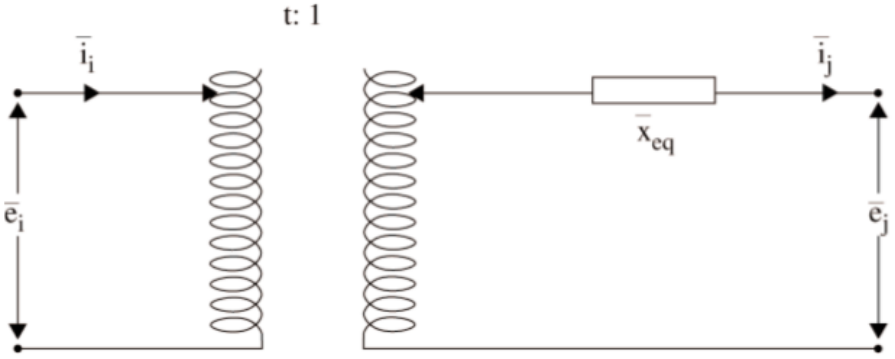

Figure 3.2: Two Winding Transformer Model[9]

The equations of two-winding transformers are similar with those of transmission line model in PowerSystems library if the tap ratio is unit one. But user can also specified the per-unit winding ratio other than one t. The connector one primary side was named as n and that of secondary side as p then the equations for the transformer models could be decried as:

$$\begin{aligned} t \times (R \times n.ir - X \times n.ii) &= n.vr - p.vr \times t; \\ t \times (R \times n.ii + X \times n.ir) &= n.vi - p.vi \times t; \\ -(R \times p.ir - X \times p.ii) &= n.vr - p.vr \times t; \\ -(R \times p.ii + X \times p.ir) &= n.vi - p.vi \times t; \end{aligned} \tag{3.6}$$

3.1.3.2 Three Windings Transformer

The three windings transformer is modeled as three two-winding transformers connected their secondary winding side together at a common star point bus as shown in Fig. 3.3. Users should

specified the per-unit between windings leakage impedances obtained from short circuit tests and the model will automatically calculate the three equivalent leakage impedances of each windings. The calculation follows the Equation 3.7. The complex off-nominal taps $t_n^{j\phi_n}(n = 1, 2, 3)$ only associate with the primary side winding which is connected to network bus, while the secondary winding side always has a tap ratio with its value equals to 1.

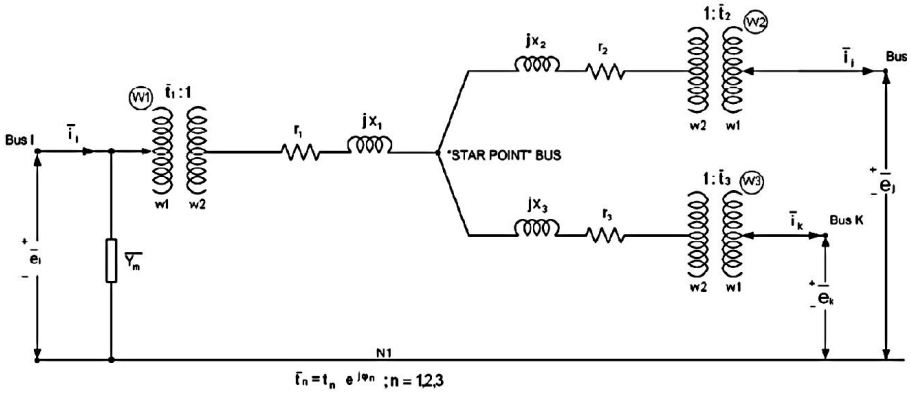

Figure 3.3: Three-Winding Transformer Model[22]

$$
\begin{aligned}
Z_1 &= \frac{Z_{12} + Z_{13} - Z_{23}}{2} \\
Z_2 &= \frac{Z_{12} + Z_{23} - Z_{13}}{2} \\
Z_3 &= \frac{Z_{23} + Z_{13} - Z_{12}}{2}
\end{aligned}
\tag{3.7}
$$

In Modelica, this construction is achieved easily, the three-winding transformer can be built by directly connecting the secondary side of three two-winding transformers together and the corresponding equations will be generated automatically.

3.1.3.3 Phase shift

The power flow through the transformer can be controlled by controlling the phase shift angle of a transformer. Introducing a shift angle to both voltage and current components in the same direction can be interpreted as viewing the original voltage and current phasor from a new coordinate which is rotated with the shift angle in reverse direction. That means, it is the same as changing the reference frame. To make it more clear, it is shown in Fig. 3.4. As a consequence, the phase shift transformer was modeled by adding the equations of Park's transformation for changing the coordinate.

$$
\begin{aligned}
A &= (-\theta_{shift} \times \frac{\pi}{180}) + \frac{\pi}{2} \\
\begin{bmatrix} Vj_r \\ Vj_i \end{bmatrix} &= \begin{bmatrix} sin(A) & cos(A) \\ -cos(A) & sin(A) \end{bmatrix} \times \begin{bmatrix} Vi_r \\ Vi_i \end{bmatrix} \\
\begin{bmatrix} Ij_r \\ Ij_i \end{bmatrix} &= - \begin{bmatrix} sin(A) & cos(A) \\ -cos(A) & sin(A) \end{bmatrix} \times \begin{bmatrix} Ii_r \\ Ii_i \end{bmatrix}
\end{aligned}
$$

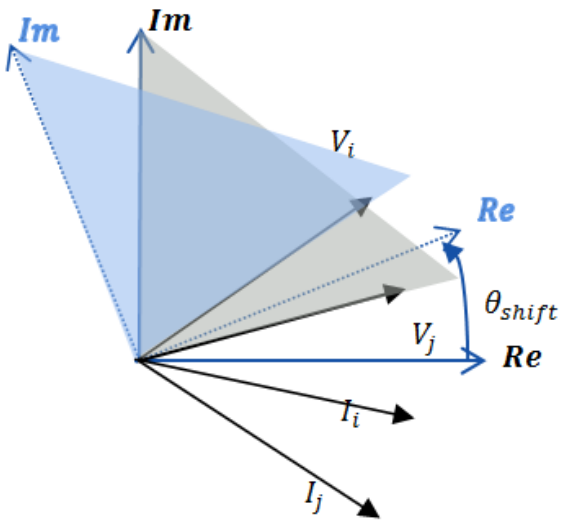

Figure 3.4: Phase shift function of transformer

3.1.3.4 On load tap changer OLTC

The tap changer function introduced in the transformer models presented previously was only statically described. By introduction on-load-tap-changer (OLTC) to the original transformer model, the bus voltage can be controlled by varied the tap ratio.

The OLTC model in this work, implements a well-established model presented in [24] [23]. It describes the tap ratio as a function of the time and of the controlled bus voltage. Only minor modification have been added to fully comply with the PSS/E model, the resulting model is described by the block diagram in Fig.3.5. It contains a dead zone block, two delay blocks, a sum block, and a quantization block.

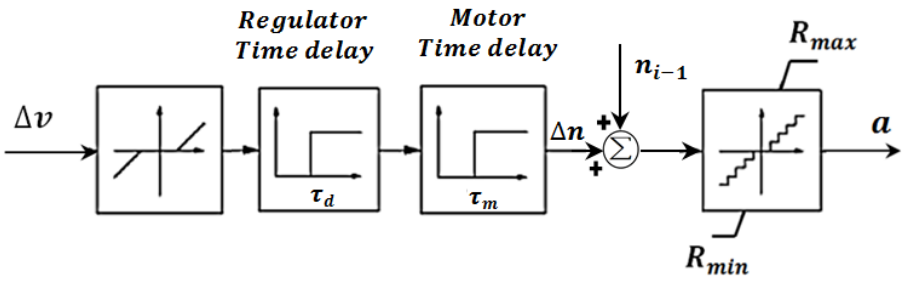

Figure 3.5: Diagram of ULTC Tap Logic[22]

The model is used to control the bus voltage to stay within the controlling band. The measured voltage is compared with the limits of the controlling band. If the voltage are out of the band by the user defined tolerance, DB, and lasting more than the delay T_D, the tap changer will react to step the tap ratio to rise or lower the voltage. The mechanical delay, T_C, for the tap changer is also considered which makes the tap ratio changes discretely. The user can define the value for a extra delay, T_{SD}. Note that delay T_{SD} must be greater than T_C to be effective. The corresponding mathematical representation is provided in the list.

Listing 3.1: Example of Parameter Decleration

```
// Detect the tap action direction
if Vmin - u > dV then
p1 = -1;
elseif u - Vmax > dV then
p1= 1;
else
p1=0;
end if;

// Count the eclipse time
if n1 > -tau and n1 < tau then
der(n1) = p1;
elseif n1 <= -tau and  p1 > 0 then
der(n1) =  p1;
elseif n1 >= tau and  p1 < 0 then
der(n1) =  p1;
else
der(n1) = 0;
end if;

// if the eclipse time is longer then the specified delay, take tap action
if n1>=tau or n1<=-tau then
action=true;
else
action=false;
end if;

// Refresh the timer if direction index change its value
x1=integer(p1);
if change(x1) then
action1=true;
else
action1=false;
end if;
when action1 then
reinit(n1,0);
end when;

//take action every TC second according to the mechanical delay
when action then
Timer2 = time;
end when;
x2 = integer((time - Timer2) / TC);
when change(x2) and action then
m = pre(m) + dtap * pre(p1);
end when;
if m>=Rmax then
y = Rmax;
elseif m<=Rmin then
y = Rmin;
else
y=m;
end if;
```

Up to now, the transformer models are completed. The parameter configuration for a simple two-winding transformer and three-winding transformer are shown as in Table 3.3 and 3.4 respectively. If the user enable the OLTC function of the transformer then there are several extra parameters need to be configured which are shown in Table 3.5.

Table 3.3: Two-winding Transformer Parameters

Parameter	Type	Description	Unit
Z_{eq}	Comp.	Equivalent impedance	p.u
t	Real	Off-nominal tap ratio	-
θ	Real	Phase shift angle	degree

Table 3.4: Three-winding Transformer Parameters

Parameter	Type	Description	Unit
Z_{12}	Comp.	Leakage impedance between winding 1 and 2	p.u
Z_{23}	Comp.	Leakage impedance between winding 3 and 2	p.u
Z_{13}	Comp.	Leakage impedance between winding 1 and 3	p.u
t_1	Real	Off-nominal tap ratio of winding 1	-
θ_1	Real	Phase shift angle of winding 1	degree
t_2	Real	Off-nominal tap ratio of winding 2	-
θ_2	Real	Phase shift angle of winding 2	degree
t_3	Real	Off-nominal tap ratio of winding 3	-
θ_3	Real	Phase shift angle of winding 3	degree

Table 3.5: OLTC model Parameters

Parameter	Type	Description	Unit
DB	Real	Dead-band of regulator	p.u
V_{max}	Real	Upper limit of the voltage control band	p.u
V_{min}	Real	lower limit of the voltage control band	p.u
R_{max}	Real	Upper limit of the off-nominal turns ratio	-
R_{min}	Real	lower limit of the off-nominal turns ratio	-
T_D	Real	Time delay of the regulator	s
T_M	Real	Mechanical time delay of the motor	s
T_C	Real	Time delay of the regulator to avoid voltage vibration	s
T_{SD}	Real	Extra user define time delay	s

3.1.4 Synchronous generator

Synchronous machine plays an essential role in power system as most of the energy is produced by different kinds of synchronous generators. In this thesis, two synchronous machine models are developed. Same assumptions with PSS/E were applied to the models. There are two kinds of synchronous generators are used in the Norwegian grid models used to represent salient pole and round pole generator.

Model Genrou represents a solid rotor generator while Gensal models the salient pole generator. Both of the two models include the effect of saturation. The equations explained in Section 3.1.4.1 to 3.1.4.3 are common for both Genrou and Gensal, but the differential equations described in Section 3.1.4.4 are different.

Every synchronous machine is modeled in its individual rotor reference frame which is rotate at the rotor speed and thus the machine quantities became static. On the other hand, all the network variables are expressed in the reference frame rotates at the synchronous speed, and this coordinate is named synchronous reference frame. The relationship is indicated in Fig. 3.6.

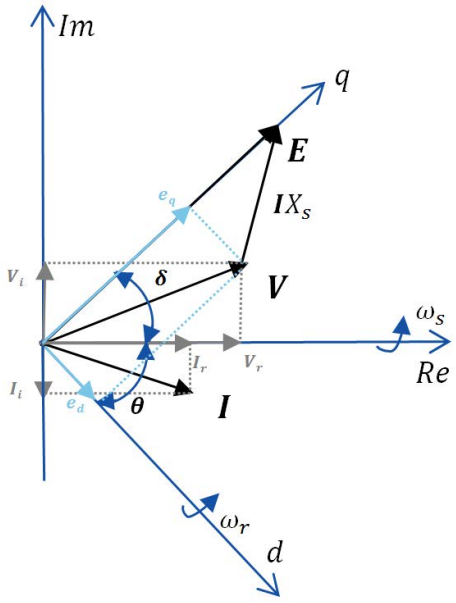

Figure 3.6: Synchronous and Rotor Coodinate

In the above figure, where generator is represented by a voltage source E behind a dynamic impedance X_s and angular spatial positions of the generator rotor shaft is defined to be the rotor angle. The synchronously rotating reference axes $\Re$-$\Im$ axes leading the dq-axes by angle $\theta = \frac{\pi}{2} - \delta$. The relationship between the quantities expressed in $\Re$-$\Im$ axes and dq-axes are as following:

$$\begin{bmatrix} V_r \\ V_i \end{bmatrix} = \begin{bmatrix} sin(\delta) & cos(\delta) \\ -cos(\delta) & sin(\delta) \end{bmatrix} \times \begin{bmatrix} e_d \\ e_q \end{bmatrix}$$

When the system is subjected to a disturbance, individual machine's rotating speed deviates from synchronous speed which causes the unbalance between power generation and consumption. The dynamic behavior of the machines are mainly affected by rotor flux linkage transients and magnetic saturation during non-steady-state with 0 to $10HZ$. The reference model from PSS/E are inherently correct representation of electromagnetic synchronizing and damping effects over the entire frequency band.

3.1.4.1 Equation of Motion

The electromagnetic torque T_e induced by the stator three phase currents can be expressed by the current and flux linkages in the dq axis:

$$T_e = \psi_d i_q - \psi_q i_d$$

While mechanical torque T_m can take the initial value or provided by corresponding turbine governor. Since T_e revolves the rotor, a unbalance between T_e and T_m can result in increasing (or decreasing) rotating energy of generator rotor and thus cause the speed deviation of the generator. To include the effect from damping torque, a term proportional to speed deviation is added. Hence, the equation of motion is:

$$\begin{aligned} 2H\frac{d\omega_r}{dt} &= T_m - T_e - D_e\frac{d\omega_r}{\omega_r} \\ \frac{d\delta}{dt} &= \omega_0 d\omega_r \end{aligned}$$

T_m = mechanical torque in p.u

T_e = electromagnetic torque in p.u

ω_r = angular velocity of the rotor,electrical. rad/s

δ = rotor angle in p.u

t = time, s

3.1.4.2 Stator voltage Equations

The elect-magnetic relationship between the generator terminal voltage, current and flux linkage is set up by stator voltage equations. With the flux transients are neglected in the models and the stator voltage is as following:

$$\begin{aligned} u_d &= -\psi_q\omega_r - R_a i_d \\ u_q &= +\psi_d\omega_r - R_a i_q \end{aligned}$$

The armature resistance R_a hasn't been taken into account in the reference models from PSS/E while the parameter is adjustable in the newly developed models but with a default value zero of R_a.

3.1.4.3 Magnetic Saturation

The input requirements for characterizing generator saturation for most commercial-grade stability programs are in terms of a parameter called S. The saturation factor is assumed to have the quadratic relation with the input voltage (or flux) as shown in Figure 3.7:

The y axis can stand for induced voltage or the flux by the field current represented by x axis, and A and B are such that the points $(1.0, S_{1.0})$ and $(1.2, S_{1.2})$ lie on the curve as shown in Figure 3.7. With the method of undetermined coefficients, the value of A and B can be calculated by solving the equations of the two points $(1.0, S_{1.0})$ and $(1.2, S_{1.2})$. Where $S_{1.0}, S_{1.2}$ are considered to be constant parameter for the generator used to determined certain saturation behavior when the stator terminal voltage is at 1.0 and 1.2 $p.u.$ as in Figure 3.7.

3.1.4.4 Electro-magnetic Equations

The difference between model Genrou and Gensal mainly lies on the differential equations which describe the electro-magnetic behavior of the models.

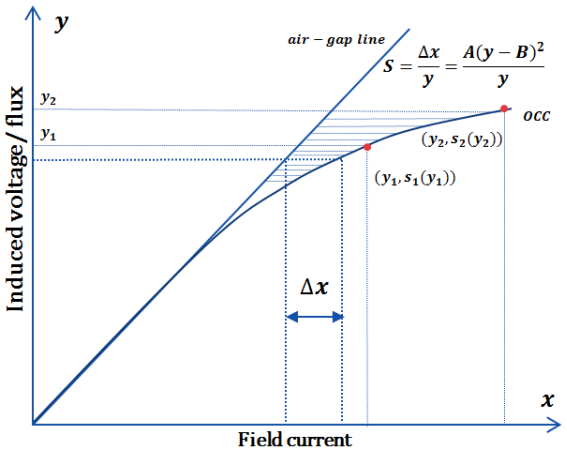

Figure 3.7: Saturation mine function

The following equations corresponding to solid rotor generator, while the equations of Gensal will be discussed later. The following equations are expressed with standard synchronous machine parameters shown in Table3.6.

Table 3.6: Standard Synchronous machine parameters of Genrou

Variable	Description	Unit
D	Damping coefficient	pu
H	Inertia constant	s
r_a	Armature resistance	pu
x_l	Leakage reactance	pu
x_d	d-axis synchronous reactance	pu
x'_d	d-axis transient reactance	pu
x''_d	d-axis sub-transient reactance	pu
x_q	q-axis synchronous reactance	pu
x'_q	q-axis transient reactance	pu
x''_q	q-axis sub-transient reactance	pu
T'_{d0}	d-axis open circuit transient time constant	s
T''_{d0}	d-axis open circuit sub-transient time constant	s
T'_{q0}	q-axis open circuit transient time constant	s
T''_{q0}	q-axis open circuit sub-transient time constant	s
s_{10}	saturation behavior parameter	-
s_{12}	saturation behavior parameter	-

$$
\begin{aligned}
\dot{E}'_q =& \frac{1}{T'_{d0}}(E_{fd} - X_{ad}I_{fd}) \\
\dot{E}'_d =& \frac{1}{T'_{q0}}(-1)(X_{aq}I_{1q}) \\
\dot{\psi_{kd}} =& \frac{1}{T''_{d0}}(E'_q - \psi_{kd} - (X'_d - X_l)i_d) \\
\dot{\psi_{kq}} =& \frac{1}{T''_{q0}}(E'_d - \psi_{kq} + (X'_q - X_l)i_q) \\
X_{ad}I_{fd} =& \frac{(X'_d - X''_d)(X_d - X'_d)}{(X'_d - X_l)^2}[E'_q - \psi_{kd} - i_d(X'_d - X_l)] \\
& + i_d(X_d - X'_d) + E'_q + S_e(|\psi''|)\psi''_d \\
X_{aq}I_{lq} =& \frac{(X'_q - X''_q)(X_q - X'_q)}{(X'_q - X_l)^2}[E'_d - \psi_{kq} + i_q(X'_q - X_l)] \\
& - i_q(X_q - X'_q) + E'_d - S_e(|\psi''|)\frac{X_q - X_l}{X_d - X_l}\psi''_q \\
\psi''_d =& \frac{E'_q(X''_d - X_l) + \psi_{kd}(X'_d - X''_d)}{X'_d - X_l} \\
\psi''_q =& \frac{-E'_d(X''_q - X_l) - \psi_{kq}(X'_q - X''_q)}{X'_q - X_l} \\
|\psi''| =& \sqrt{(\psi''_d)^2 + (\psi''_q)^2} \\
\psi_d =& \psi''_d - X''_d i_d \\
\psi_q =& \psi''_q - X''_q i_q
\end{aligned}
$$

For salient pole generator, there are in total three rotor circuits. In order to represent the model in detail, one state variable is introduced for each of the rotor circuit. Additionally, the magnetic saturation is only account for d axis. The following equations can is the correct representation of its electro-magnetic behavior. The standard parameters is shown in Table3.7.

Table 3.7: GENSAL

Variable	Description	Unit
T'_{do}	d-axis transient open-circuit time constant	sec
T''_{do}	d-axis sub-transient open-circuit time constant	sec
T''_{qo}	q-axis sub-transient open-circuit time constant	sec
H	Inertial,H	sec
D	Speed damping	
X_d	d-axis reactance	p.u.
X_q	q-axis reactance	p.u.
X'_d	d-axis transient reactance	p.u.
X''_d	d-axis sub-transient reactanc	s
X_l	leakage reactance	s
$S(1.0)$	Saturation factor	p.u.
$S(1.2)$	Saturation factor	p.u.

$$
\begin{aligned}
\dot{E}'_q =& \frac{1}{T'_{d0}}(E_{fd} - X_{ad}I_{fd}) \\
\dot{\psi_{kd}} =& \frac{1}{T''_{d0}}(E'_q - \psi_{kd} - (X'_d - X_l)i_d) \\
\dot{\psi''_q} =& \frac{-1}{T''_{q0}}(\psi''_q + (X'_q - X''_q)i_q) \\
X_{ad}I_{fd} =& \frac{(X'_d - X''_d)(X_d - X'_d)}{(X'_d - X_l)^2}[E'_q - \psi_{kd} - i_d(X'_d - X_l)] \\
& + i_d(X_d - X'_d) + E'_q + S_e(E'_q)E'_q \\
\psi''_d =& \frac{E'_q(X''_d - X_l) + \psi_{kd}(X'_d - X''_d)}{X'_d - X_l} \\
\psi_d =& \psi''_d - X''_d i_d \\
\psi_q =& \psi''_q - X''_q i_q
\end{aligned}
$$

3.2 Nonelectrical Element

A grid model contains not only the electrical components which participate in the power flow directly but also different control systems which regulate the control signal of the generator and therefore have a strong influence on the dynamic behavior of the system.

3.2.1 Excitation System

The direct field current of the generator has a directly impact on its terminal bus voltage. This field current is supplied and controlled by the excitation system. This system take the measured voltage magnitude from generator's terminal bus and compare it with the set point, and then it will modify the field current of the generator to get desire output voltage from the generator.

There are different types of exciter models. According to the structure of their power-supply circuit, they could be sorted into three main branches: Direct Current Commutator Exciters **(DC exciter)**, Alternator Supplied Rectifier Excitation Systems **(AC exciter)** and **Static Excitation Systems**.

While DC exciter can be future identified as **separately excited exciter** or **shunt excited exciter**. The circuits of these two types of DC exciters are shown in the following figures. In the figures R is the field resistance, L is the unsaturated inductance and V is the output from voltage regulator. On the other hand, normally AC exciters are separated exited exciters, and because their only load is a rectifier, their magnetic behavior can be modeled in the same way as that of DC exciters with acceptable accuracy. Thus the following discussion would mainly focus on DC exciter, since AC exciter can be represented by the same model used to describe separately excited DC exciter.

The equations for the separately excited exciter is shown as in Equation 3.8. To take into account the saturation effect, the saturation factor is included in the equation. The calculation of S_e follows the same definition as it is described in Section 3.1.4.3, the only difference is that the S_e is now a function of field voltage E_{fd} instead of the flux linkage. To specified the certain saturation behavior, two points lying along the saturation curve must be specified as parameters$(E_1, S_e(E_1)), (E_2, S_e(E_2))$.

$$
\frac{L}{R}\frac{dE_{fd}}{dt} = \frac{V}{R} - E_{fd} - S_e E_{fd} \tag{3.8}
$$

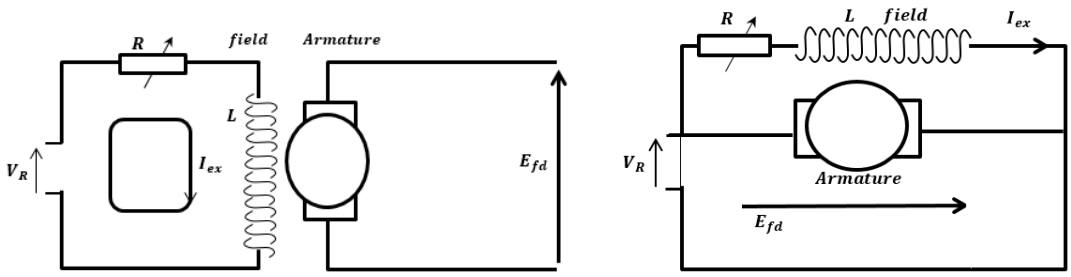

(a) separately excited exciter (b) shunt excited exciter

Figure 3.8: Equivalent excited circuit for Exciter

By setting:

$$\begin{aligned} T_e =& \frac{L}{R} \\ K_e =& 1 \end{aligned}$$

Practically, field resistance R is an adjustable value but is assumed that the adjustment has been done for each new per-event steady-state condition. Thus the recalculation of R must be included in the initialization stage and then it is considered to remain constant during dynamic simulation. Since the value of R might vary little around unity, T_e can be taken as constant.

For shunt excited exciter, since the power source provide the power to both field and armature circuit of the excitation system, the equation remains almost the same as before but with an additional term in the right hand side and it is shown as in Equation 3.9.

$$\frac{L}{R}\frac{dE_{fd}}{dt} = \frac{V}{R} - (1 - \frac{1}{R})E_{fd} - S_e E_{fd} \tag{3.9}$$

To simply the equation, we set:

$$\begin{aligned} T_e =& \frac{L}{R} \\ K_e =& 1 - \frac{1}{R} \end{aligned}$$

Since R is around unity, thus K_e will be significantly influenced by R so that it must be adjusted to an appropriate value during initializing. The models developed in this work adopt the same configuration as the PSS/E model. It is possible to specify the value manually or let the model calculate the value itself. The model can handle the calculation of K_e automatically and also the relative parameters V_{rmax} and V_{rmin} if they are specified as zero by users. The logic for calculation is shown as below.

$$K_e = \frac{V_{rmax}}{10E_{fd}} - S_e(E_{fd}) \qquad K_e = 0$$

$$\begin{cases} V_{rmax} &= S_e(E_2)E_2 + K_e & K_e > 0, V_{rmax} = 0 \\ V_{rmax} &= S_e(E_2)E_2 & K_e <= 0, V_{rmax} = 0 \end{cases}$$

The equations derived in previous section only cover the part of exciter model for excitation system, however, there are also voltage sensor and regulator should be modeled. But the way of modeling them are typical and relative simpler then that of exciter, thus the discussion of them are dropped. The models developed in this thesis are **IEEET1**, **IEEET2**, **SEXS** and **SCRXS**.

The equations can be simplified and be expressed as transfer block diagrams.

IEEET1 is an IEEE standard excitation system model which could represent either a DC or a AC type system depends on the value of parameter K_e. The model also take into account the power supply limit, the stabilization feedback loop and the saturation effect. The transfer diagram of the model is shown in Fig. 3.9

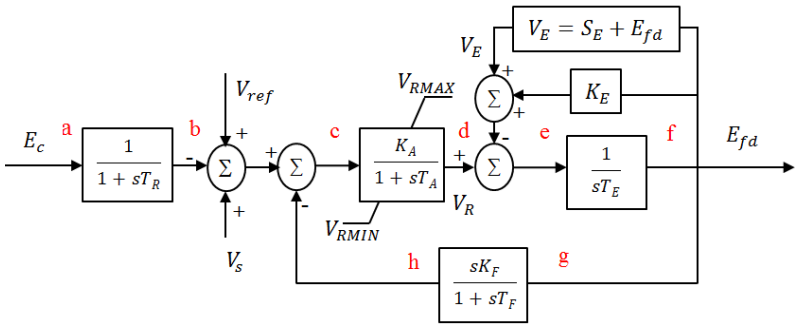

Figure 3.9: Block Diagram of IEEET1

When it is used to represent DC type excitation system, it is recommended that K_e, V_{rmax}, V_{rmin} should be set to be zero and left the model calculate the values automatically. On the other hand, when it is used to model a AC type excitation system, K_e should be set to unity while still it is recommended to let the model itself calculate the values for V_{rmax}, V_{rmin}. The parameters of the model is shown in the Table 3.8.

Table 3.8: IEEET1

Variable	Description	Unit
T_R	Voltage sensor time constant	sec
K_A	Voltage regulator gain	sec
T_A	Voltage regulator time constant	sec
V_{RMAX}	Power source upper limit	sec
V_{RMIN}	Power source lower limit	
K_E	Exciter equivalent gain	p.u.
T_E	Exciter equivalent time constant	p.u.
K_F	Feedback loop equivalent gain	p.u.
T_F	Feedback loop equivalent time constant	s
E_1	Field voltage value	p.u.
$S_E(E_1)$	Saturation factor	p.u.
E_2	Field voltage value	p.u.
$S_E(E_2)$	Saturation factor	p.u.

As we have discussed previously, the system mode should be initialized before switching to dynamic analysis. After the initialization of the generator, we can get the initial values of variables at the boundary of a generator which interfaces with the excitation system. As a result, each block is initialized by assign a initial value to its state which contributes to make the whole excitation system satisfies the boundary conditions. In order to properly initialize the states, it is needed to apply inverse *Laplace* transformation on the given block diagram. For the sake of analysis, the input and output of each block is identified by a letter. After transformation, the following equations is obtained:

$$
\begin{aligned}
a &= b + T_R\dot{b} \\
K_A c &= d + T_A\dot{d} \\
e &= T_E\dot{f} \\
K_F\dot{g} &= h + T_F\dot{h}
\end{aligned}
$$

When it is steady state, the time derivative of all the states are zero,and the output of the exciter should be the same as the field voltage at steady state. Without compensate circuit, the input of the exciter should be the initial value of measured generator bus voltage.

$$
\begin{aligned}
a_0 &= b_0 = V_{t0} \\
K_A c_0 &= d_0 \\
e_0 &= h_0 = 0 \\
f_0 &= E_{fd0}
\end{aligned}
$$

d_0 which is the initial regulator output V_{R0} can be calculated as following. And the reference voltage is set as:

$$
\begin{aligned}
V_{R0} &= (S_e(E_{fd0}) + 1 + K_E)Efd0 \\
V_{ref} &= \frac{V_{R0}}{K_A} - V_{S0} + V_{t0}
\end{aligned}
$$

IEEET2 is also an IEEE standard excitation system model. Differing from IEEET1, IEEET2 take the source used for the excitation system stabilizing feedback as proportional to the control element output, while IEEET1 takes a stabilization signal proportional to the main output E_{fd} of the exciter. The block diagram for the IEEET2 is shown in Figure3.10. And the parameter sheet is shown in Table3.9.

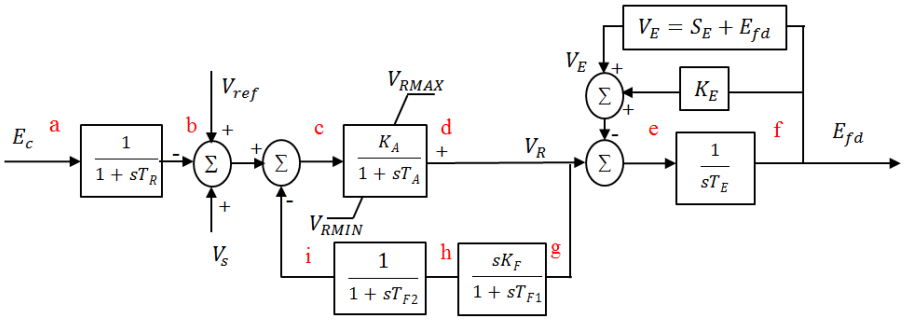

Figure 3.10: Block Diagram of IEEET2

IEEET2 can be initialized by following the same calculation procedure as before and the initial value of each states are:

$$
\begin{aligned}
a_0 &= b_0 = V_{t0} \\
K_A c_0 &= d_0 \\
e_0 &= h_0 = i_0 = 0 \\
f_0 &= E_{fd0} \\
V_{R0} &= (S_e(E_{fd0}) + 1 + K_E)Efd0 \\
V_{ref} &= \frac{V_{R0}}{K_A} - V_{S0} + V_{t0}
\end{aligned}
$$

Table 3.9: IEEET2

Variable	Description	Unit
T_R	Voltage sensor time constant	sec
K_A	Voltage regulator gain	sec
T_A	Voltage regulator time constant	sec
V_{RMAX}	Power source upper limit	sec
V_{RMIN}	Power source lower limit	
K_E	Exciter equivalent gain	p.u.
T_E	Exciter equivalent time constant	p.u.
K_F	Feedback loop equivalent gain	p.u.
T_{F1}	Feedback loop equivalent time constant	s
T_{F2}	Feedback loop equivalent time constant	s
E_1	Field voltage value	p.u.
$S_E(E_1)$	Saturation factor	p.u.
E_2	Field voltage value	p.u.
$S_E(E_2)$	Saturation factor	p.u.

SEXS is a good presentation of general well tuned excitation system without focusing on any specific types, if the detail design of the excitation system is unknown. It include a basic representation of the excitation power source (with the gain K, time constant T_e and limits E_{max} and E_{min}) and the transient gain reduction (with time constant T_A and T_B). T_A and T_B are used to specified desired dynamic behavior with high steady-state gain. The The transfer block of SEXS is quite simple which is shown as in Figure3.11. The parameter is in Table3.10. Similarly, by substitute all time derivatives to be zero, the initial values are obtained:

$$a_0 = b_0 = \frac{c_0}{K}$$
$$c_0 = E_{fd0}$$
$$V_{ref} = \frac{E_{fd0}}{K} - V_{S0} + V_{t0}$$

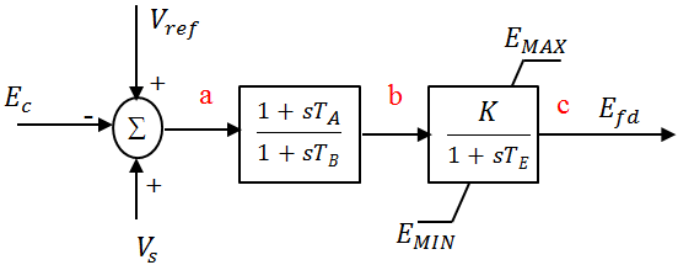

Figure 3.11: Block Diagram of SEXS

Table 3.10: SEXS

Variable	Description	Unit
T_A/T_B	ratio of Power source transient gain reduction	p.u.
T_B	Power source transient gain reduction	sec
K	Power source gain	sec
T_E	Power source time constant	sec
E_{MAX}	Power source upper limit	p.u.
E_{MIN}	Power source lower limit	p.u.

SCRX is also a general representation of the excitation system. But compare to SEXS, model SCRX can be better representation of those AC excitation system connected the power supply thought a rectifier bridge. The power supply can come from a generator terminal voltage or a auxiliary power plan, and model SCRX can distinguish between these two. Further more model SCRX include a logic named "Negative current logic" to represent different protect strategies for the forward rectifier bridge, and it could be either a reversed bypassing diode or a controlled rectifier excitation systems. The circuit for the system with a bypassing diode is shown in Fig. 3.12.

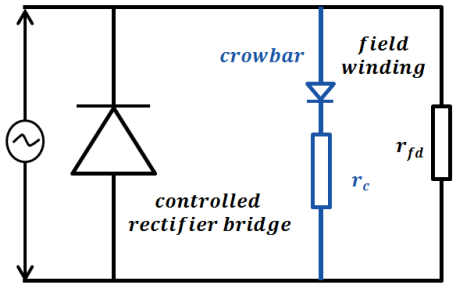

Figure 3.12: Equivalent circuit of SCRX with *crowbar*

The equation below describe the above circuit in the situation where the field voltage of the generator is higher than the AC power supply leading to a negative current flowing through the bypassing diode.

$$E_{fd} = \frac{R_C}{r_{fd}} X_{ad} I_{fd} \tag{3.10}$$

On the other hand, the circuit for the system equipped with controlled rectifier excitation system can also be represented as in Fig. 3.12 but without the resistance which means r_c equals to zero. Thus under the situation discussed above, for this circuit it becomes:

$$E_{fd} = 0 \tag{3.11}$$

Thus for SCRX, negative current logic can be summarized as:

$$E_{fd} = \begin{cases} V_{crow} & X_{ad} I_{fd} < 0 \\ V_R & \text{otherwise} \end{cases}$$

$$V_{crow} = \begin{cases} \frac{R_C}{r_{fd}} X_{ad} I_{fd} & \frac{R_C}{r_{fd}} > 0 \\ 0 & \frac{R_C}{r_{fd}} = 0 \end{cases}$$

The block diagram of the model is shown in the Fig. 3.13 and the parameters are listed in the following table.

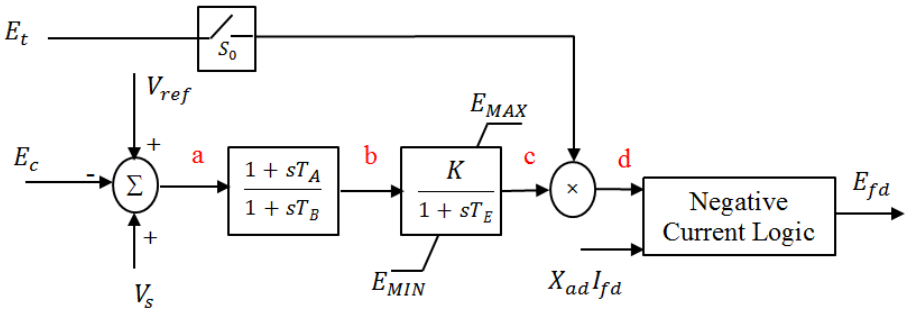

Figure 3.13: Block Diagram of SCRX

Table 3.11: SCRX

Variable	Description	Unit
T_A/T_B	ratio of Power source transient gain reduction	p.u.
T_B	Power source transient gain reduction	sec
K	Power source gain	sec
T_E	Power source time constant	p.u.
E_{MAX}	Power source upper limit	sec
E_{MIN}	Power source lower limit	
C_{switch}	Indicator shows generator bus fed mode or separately power supply)	-
r_c/r_{fd}	ratio of crowbar and field winding resistor	p.u.

When calculate the initial states of the model, it is reasonable to eliminate the "Negative current logic", If the rectifier system is fed by an auxiliary bus plan, then the initialization procedure of SCRX is the same as that of model SEXS. However, when it is used to represent a generator terminal bus fed rectifier system, the initialization should also consider the initial value of the bus fed signal.

$$c_0 = \frac{E_{fd0}}{Et0} \tag{3.12}$$

$$V_{ref} = \frac{E_{fd0}}{KEt0} - V_{S0} + V_{t0} \tag{3.13}$$

3.2.2 Power System Stabilizer

To compensate the negative effect of the excitation systems on the damping torque, a power system stabilizer (PSS) is added to the generator. The function of PSS is to introduce a supplementary signal into the voltage regulator with appropriate phase and gain adjustments to provide additional damping which will be sufficient to cancel the negative effect of the exciters.

IEEEST is a quite general model, a wild range of information can be pick up as input signal, *e.g.*, active power, speed deviation, or voltage magnitude. In PSS/E the user should specified the source for input signal with which quantity. It can be either from generator terminal or a remote bus. However in Dymola, one just need to put a sensor to measure the desired information, and input it to IEEEST through connector directly.

The transfer function of IEEEST is shown in Fig. 3.14 which consists of a notch filter, two lead-lag blocks and a washout block. The parameter used in the diagram is explained in Table 3.12. By appropriately specifying the time constants of the two lead-lay blocks, desired phase lead can be introduced to that of the input signal. Except the block of wash-out, all of the other block can be

bypassed by setting the relative parameters to be zero. The effect of the washout block may be canceled by setting T_5=T_6=20.

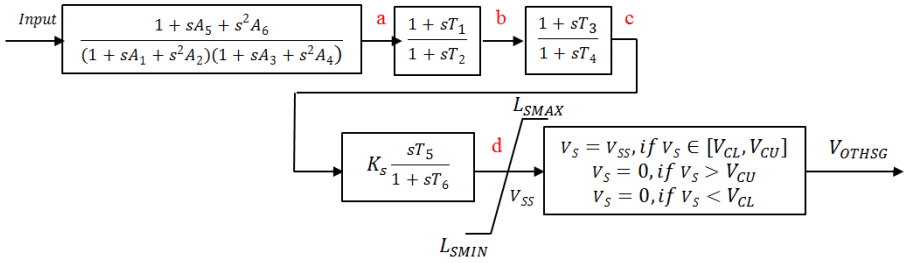

Figure 3.14: Block Diagram of IEEEST

$$a_0 = P_{t0}, V_{t0} \ \ or \Delta\omega(=0)$$
$$a_0 = b_0$$
$$b_0 = c_0$$
$$d_0 = 0$$

Table 3.12: IEEEST

Variable	Description	Unit
A_1	Filter coefficient	-
A_2	Filter coefficient	-
A_3	Filter coefficient	-
A_4	Filter coefficient	-
A_5	Filter coefficient	-
A_6	Filter coefficient	-
T_1	Lead time constant	sec
T_2	Lag time constant	sec
T_3	Lead time constant	sec
T_4	Lag time constant	sec
T_5	Washout time constant	sec
T_6	Washout time constant	sec
K_S	Stabilizer gain	p.u.
L_{SMAX}	Upper limit	p.u.
L_{SMAX}	Lower limit	p.u.
V_{CU}	Upper limit(if zero then ignored)	p.u.
V_{CL}	Lower limit(if zero then ignored)	p.u.

STAB2A is designed specially for modeling the stabilizer which take the generator electrical power as supplementary signal. The block diagram and the parameter is provided as following. Following the same initialization procedure, one can find that the initial values of all of the states are zero.

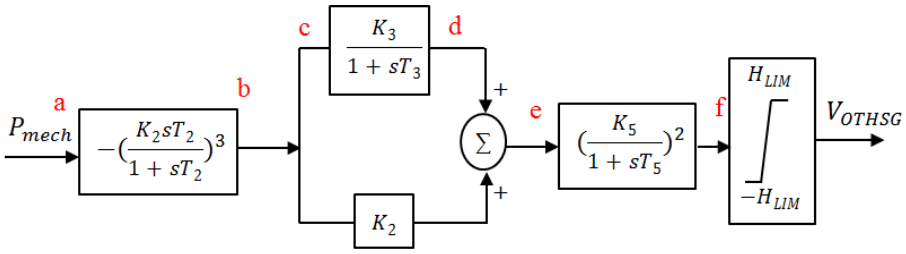

Figure 3.15: Block Diagram of STAB2A

Table 3.13: STAB2A

Variable	Description	Unit
K_2	Block gain	-
T_2	Block time constant	sec
K_3	Block gain	-
T_3	Block time constant	sec
K_4	Block gain	-
K_5	Block gain	-
T_5	Block time constant	sec
H_{LIM}	Output limit	p.u.

3.2.3 Governor System

In power system network, a balance between the real power generation and the load demand should be maintained continuously. The frequency or the rotational speed of the generator is influenced by the power generation directly and the relation is ruled by the swing equation. Therefore, any increase in load demand would tend to cause the frequency to decrease while any decrease in load would tend to cause the frequency to increase.

It has been mentioned that each generator has its own frequency, and during normal operation it is required that all the generators should stay synchronous. As a result, there is a need to equip a governor with generator. A governor is a device used to measure and regulate the frequency (speed) of a generator. Basically it contains two system the first one is the speed governing system which will detect the speed deviation and react to control the vales or the gates in turns the input source energy to the second part the turbine system which will transfer the mechanical power to the electrical power.

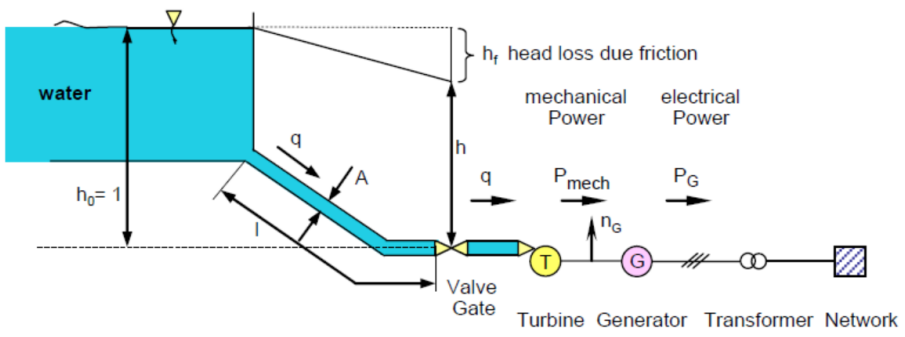

Figure 3.16: Hydro Turbine Diagram[25]

h_0	static head of water column
l	penstock length
A	penstock area
q	urbine flow rate
h	head at the turbine admission
ω_G	generator speed

The diagram of a hydraulic turbine system is shown in the above figure. The water in the reservoir falls down from the penstock from which it gains kinetic energy. This energy is harvested by the hydro turbine and converted into mechanical power and then transmitted to the shaft of the generator. The governor of the turbine control the gate and thus the water flow.

Due to the inertia of the water, opening the gate will not immediately results in an increased flow of water when reaching the turbine. It is because that at the instance of opening the gate, there will be a transient reduction of the water pressure which will cause a decrease in mechanical power output. This phenomenon is called the water column characteristic. The *acceleration of water column* can accounted as a nonlinear function between the velocity of the water and the change in the head. [6]. The block diagram in Fig. 3.17 completely describe the nonlinear water column and turbine characteristic.

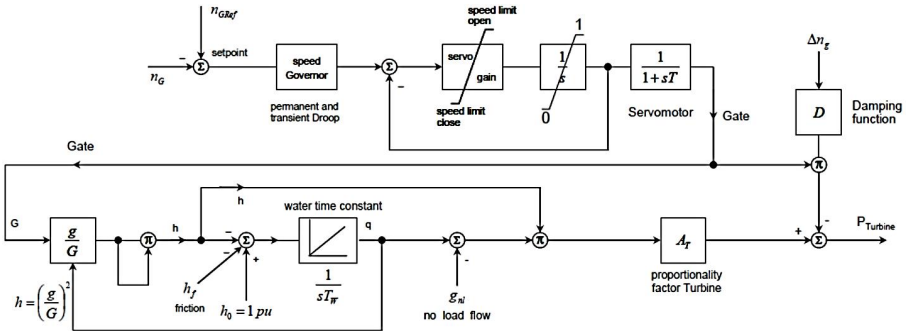

Figure 3.17: Hydro Turbine Diagram 2[25]

Different representations of the hydraulic system result in various models for hydroelectric plans. In this thesis two of them have been developed. One is a linear model which is an IEEE standard governor model, IEEESGO and another is a nonlinear model HYGOV.

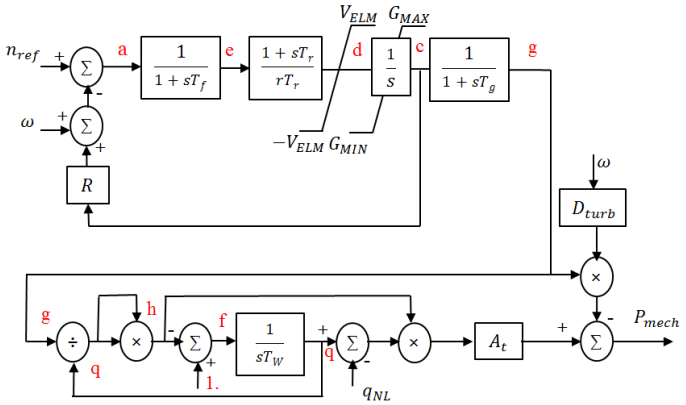

Figure 3.18: Block Diagram of HYGOV

HYGOV represents a straightforward hydroelectric plant governor, with a simple hydraulic representation of the penstock with unrestricted head race and tail race, and no surge tank [9]. The diagram of the model is shown in Fig. 3.18 which drops the part representing The head loss due to friction h_f.

Table 3.14: HYGOV

Variable	Description	Unit
R	Permanent droop	p.u
r	Temporary droop	p.u
T_r	Governor time constant	sec
T_f	Filter time constant	sec
T_g	Servo time constant	sec
$\pm$ VELM	Gate velocity limit	p.u.
G_{MAX}	Maximum gate limit	p.u.
G_{MIN}	Minimum gate limit	p.u.
T_W	Water time constant	sec
A_t	Turbine gain	p.u.
D_{turb}	Turbine damping	p.u.
q_{NL}	No load flow	p.u.

A_t is the turbine gain which relate the ideal gate opening (from no load to full load) to real gate opening (from fully closed to fully open). The water starting time Tw represents the time required for the water to reach a flow rate q in the penstock starting from the height h at zero speed. The value is depending on the loading level which is inconvenient for performing the simulation. As a result, the parameter Tw instead of Tw is used in the model which is the value of Tw but calculated using per unit base flows and heads. Different from Tw, Tw is a fixed value for a given turbine-penstock unit and at the same time taking into account the dynamic changes automatically. For detail of the changing base procedure, one can refer to [6].

To initialize the model, following calculation should be performed. Where at steady state, there is no speed deviation and the model should provided the desired mechanical power to the generator which is obtained from initialization of the machine. By substituting the time derivatives of the variables to be zero:

$$
\begin{aligned}
&a_0 = e_0 = d_0 = 0 \\
&c_0 = g_0 \\
&(\frac{q_0}{g_0})^2 = 1 \\
&h_0 = 1 \\
&f_0 = 0 \\
&q_0 = \frac{P_{mech0}}{A_t h} + q_{NL}
\end{aligned}
$$

The it is possible to calculate the desired set value of the speed reference by following equation.

$$n_{ref} = R(\frac{P_{mech0}}{A_t h} + q_{NL})$$

IEEESGO is a general-purpose turbine-governor model. It either be a good representation of a reheat steam turbine or an approximate representation of a simplified hydro plant. The block diagram, parameter sheet and initial procedure are:

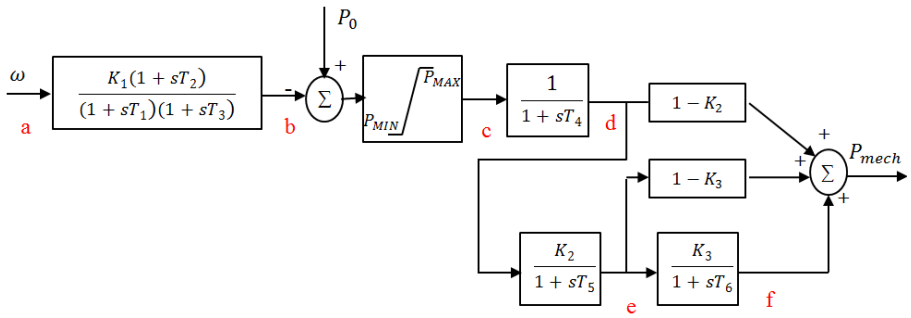

Figure 3.19: Block Diagram of IEESGO

$$
\begin{aligned}
a_0 &= 0 \\
b_0 &= K_1 a_0 \\
c_0 &= P_0 \\
d_0 &= c_0 \\
e_0 &= K_2 d_0 \\
f_0 &= K_3 e_0
\end{aligned}
$$

Table 3.15: IEESGO

Variable	Description	Unit
T_1	Controller lag	sec
T_2	Controller lead compensation	sec
T_3	Governor lag	sec
T_4	Delay due to steam inlet volumes associated with steam chest and inlet piping	sec
T_5	Re-heater delay including hot and cold leads	sec
T_6	Delay due to IP-LP turbine, crossover pipes,and LP end hoods	sec
K_1	Maximum gate limit	p.u.
K_2	Minimum gate limit	p.u.
K_3	Water time constant	sec
P_{MAX}	Upper power limit	p.u.
P_{MIN}	lower power limit	p.u.

4 Model Validation

It is necessary to perform complete validation tests in order to check that there are high degree of similarity between the performance of the models and the reference models. The validation procedure and the analysis of the results are described in the chapter. The validation steps could be summarized as three steps:

1. **Design the structure and the perturbation of the test system in PSS/E** The test system should be designed as simple as possible for the sake of control variables, however, at the same time the system should be as complete as possible thus the dynamic of which can reflect all the feature of the components needed to be validated.

2. **Record the power flow results and dynamic responds of the test system in PSS/E** As it has be mentioned previously, all the components are initialized to match the equilibrium calculated from power flow. Power flow is not available in Dymola, thus it is necessary to take the PSS/E PF results as input parameter for the system in Dymola. It is recommended to record the power and voltage information for all the bus which equipped with generator or composite load. After that, simulate the system to get the dynamic responds. For the electrical components, the focus should be put on complex power and voltage information, while for the control system, the focus should be put on the real input and output of the components.

3. **Build the identical system in Dymola and putting in the parameter for each component** It is recommended that an individual data record should be built for each test model especially for large test system. Since typing parameters for the whole system manually would be time consuming and problematic, and it would be difficult for one to check if there is any mistake. For the part of data management, one can refer to Dymola manual, and it will not be repeated here.

4. **Implement the same perturbation cases in Dymola** It is the critical step during the validation that the same perturbation should be implemented for the system in Dymola. To achieve it, detail of the method of applying perturbation in PSS/E should be fully studied. For example, the way of applying load variation, step respond test of control devices etc.

5. **Simulation the system in Dymola and record the system response.** During this step, it is recommended that the same simulation parameters are applied. The essential parameters are the simulation interval and the solver method. Simulation interval is the sampling interval of the system response, with different interval, different points from system response curve will be recorded. While different solver methods apply various order of Taylor series to approximate the real solution of the system response which will influence the accuracy of the simulation results. The transient behavior of the dynamic components are of prime interest thus the focus is put on the transient response of different perturbations. The setup of the test systems and the applied disturbance are explained in turns. The parameters used in the test systems are provided in Appendix.

4.1 Small-Scale Power System Tests

As it has been mentioned that, for the sake of controlling variables, the validation tests should start from the simplest system contained the lowest degree of dynamics. A single generator model is first validated and then the tests processed by introduced the control devices. The basic scenario used for study the transient performance of generator and its regulator is shown in the diagram 4.1

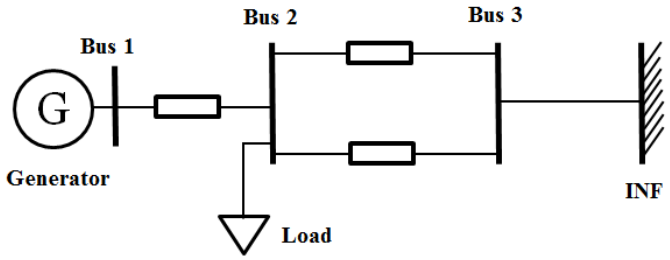

Figure 4.1: Test system diagram

where the generator is delivering power through one transmission line to a composite load and then through two parallel lines to a large system in remote area. The power flow results are shown in Table 4.1. The frequency and the system base used in all test system is 50Hz and 100MVA respectively. The unit of the angle is degree, while all of the other value are expressed in per unit on system base. Since each generator and its regulators are on machine base, there is needed for changing base. This is achieved by explicitly introducing the bus which changing base for current components directly at the terminal of generators. Note that positive sign is used when the power is injected into the bus node.

Table 4.1: Power Flow Result

Bus	Voltage	Angle	Active power	Reactive power
1	0.999999	4.0463	0.399989	0.054165
3	1	-3.00563e-7	0.100184	0.080064

The power flow results are picked up from PSS/E. As it has been described in section **??**, the generator terminal quantities such as the phasor of voltage and apparent power served as input variables for initialization calculation. The accuracy of the power flow results have a direct affect on the correctness of the initialization. The more the complexity of the system, the higher the tolerance of power flow input values are required.

Validation results of the components should demonstrate both the correctness of the initialization and the transient behavior of the dynamic components under disturbance. In order to check the initialization results, all of the system are running under stationary state for two seconds. After that, different perturbations are applied to force the systems into transient. The transient disturbances are illustrated in Fig. 4.2(a) to 4.2(d), they could be a three phase to ground fault in the middle of the transmission lines or at the terminal bus of generator. One can also apply load variational or a step change of regulator's reference value to the system. All of the perturbation were modeled in the same way as they are in PSS/E.

Within in a period of a few seconds after the disturbance, the system might suffer from large excursions of generator rotor angles, power flows, bus voltages, and other system variables. The dynamic behavior of the power system during this time range related to the dynamic introduced

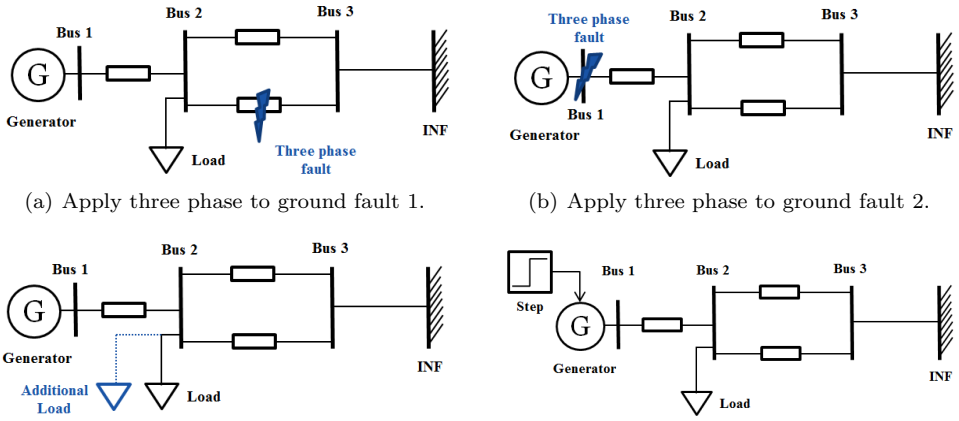

(a) Apply three phase to ground fault 1.

(b) Apply three phase to ground fault 2.

(c) Apply load variation.

(d) Apply regulator referenc step.

Figure 4.2: Different perturbation cases.

by the rotor inertia storage energy, the field electromagnetic transients, and the controls of generators. Thus the signal such as generator speed deviation $\Delta\omega$, the bus voltage magnitude, and the injected active and reactive power P and Q of generator are recored and compared.

When there exist regulators in the system, the output quantities of those equipments are compared and analyzed. Specially, the limit of regulation should be broken if there exist one, so that one can make sure that the system react in the same way when regulators hits their limits. The simulations were continuing until the transient period of the system dies out completely in order to make sure that when transient has died out, the test systems built in Dymola and PSS/E can return to the same equivalent operation point. But in most of the cases, the new steady state is achieved around $20s$, thus the simulation time length could be set to $20s$. The figures attached in this chapter were shown with zoom in action where the time length in the figures might be less than $20s$.

Since in PSS/E, except generator, all the dynamic devices can not be tested individually, thus different components are combined and tested in groups. Certain perturbation from Fig. 4.2 are applied to active the specific functions of the components such as the saturation function of detail exciter model (IEEET1 and IEEET2), the negative current logic of SCRX, and the no-windup and windup limits within HYGOV. The combinations are summarized as in Table 4.2.

Table 4.2: Combination of Dynamic Devices

No.	Dynamic Device
1	Genrou
2	Gensal with two-winding transformer
3	Genrou+IEEET2+IEESGO
4	Gensal+SCRX+HYGOV
5	Gensal+IEEEST+SEXS
6	Genrou+IEEET1+STAB2A+LFDRAL
7	Genrou+IEEET1+STAB2A with three-winding transformer

For the sake of controlling variables, the setting of all simulations performed in PSS/E and Dymola are chosen to be as similar as possible. The settings are listed as below, beside that all the variables which were picked up to be recorded and compared are also listed out. The error in percentage

the normal distribution of the absolute difference are also plotted. But due to the limit of the space, only the plots of error for 3_{rd} case are attached in this chapter.

Table 4.3: Dynamic setting in PSS/E version 33

Acceleration	0.5
Network solution iterations	25
Tolerance	0.0001
Island frequency acceleration	1.000
Island frequency tolerance	0.0005
Time step	$5ms$
Frequency filter	0.0333
Delta threshold intermediate	0.04
Delta threshold Island frequency	0.016667
Network frequency dependence	off
Plot every time step	-

Table 4.4: Dynamic setting in Dymola

Quantities at generator terminal	Part 1
Algorithm	$Rkfix2$
Tolerance	0.0001
Time step	$5ms$
Output interval length	0.005
Number of output interval	5000
Quantities at generator terminal	Part 2
Algorithm	$Rkfix4$
Tolerance	0.0001
Time step	$5ms$
Number of output interval	6000

Table 4.5: Variables to be recorded

Quantities at generator terminal	symbol
speed deviation	ω
terminal voltage	V_t
generated active	P_{gen}
generated reactive power	Q_{gen}.
Quantities at load bus	symbol
the magnitude of bus voltage	θ_{load}
the angle of bus voltage	V
consumed active power	P_{load}
consumed reactive power	Q_{load}.
output of regulators	symbol
governor output, the mechanical power of generator	P_m.
exciter output, the field voltage of generator	E_{fd}.
stabilizer output	V_{othsg}.

The test system for components like two-winding and three-winding transformers are different from the basic one.

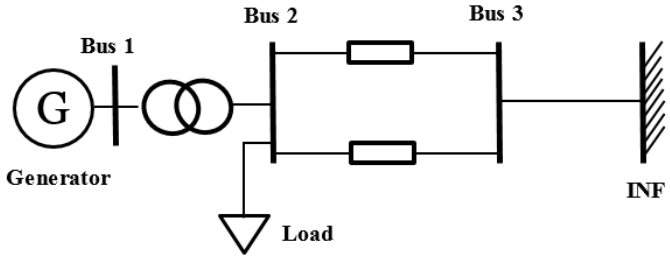

Figure 4.3: Test system diagram for two-winding transformer with phase-shift

Table 4.6: Power flow result for the system including three-winding transformer

Bus	Voltage	Angle	Active power	Reactive power
1	1	0.293027	0.10083	0.20187
2	0.977048	-0.569458	0.49253	0.097037
3	1	0	0.105725	0.231136

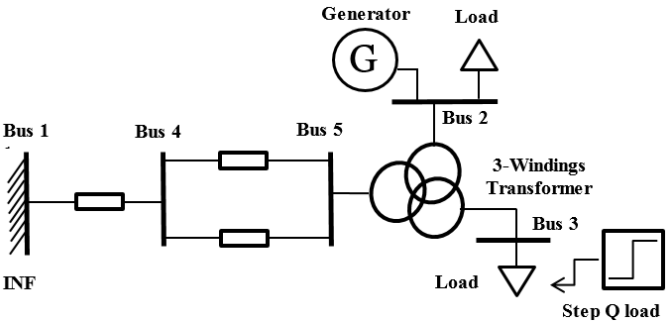

Figure 4.4: Test system diagram for three-winding transformer with OLTC

Table 4.7: Power flow result for the system including two-winding transformer

Bus	Voltage	Angle	Active power	Reactive power
1	1	0	0.10083	0.20187
2_{load}	0.9978	0.08	0.4	0.4
$2_{Generator}$	0.9978	0.08	0.1	0.5
3	0.9962	-0.12	0.4	0.1

4.1.1 Validation of Genrou

In this section, validation results of round role generator model were analysis. Below are the diagram for the test used in Dymola and a list of the simulations performed during testing. Since the initialization of generator model is the start point of dynamic simulation, the accuracy of the initial values should be check carefully. The results of initialization were recorded in Table 4.9.

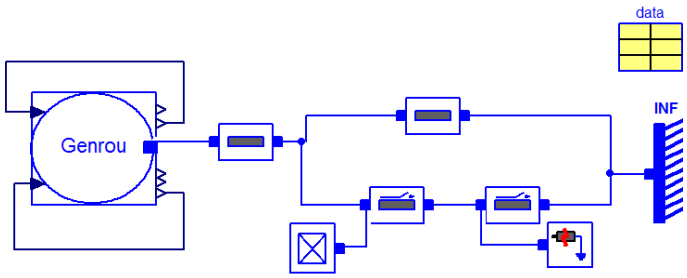

Figure 4.5: Diagram in Dymola of the GENROU test system.

Table 4.8: List of simulations

Step	Scenarios
1.	running under steady state for 2 seconds.
2.	Vary the system load with constant P/Q ratio Fig. 4.2(c).
3.	After 0.1s later, the load was restored to its original value .
4.	Run simulation to 10s.
5.	Apply three phase to ground fault as shown in Fig. 4.2(a).
6.	After 0.15s later, the fault was cleared by tripping the line.
7.	Run simulation until 20 seconds.

Table 4.9: Initialization

No.	Quantities	PSS/E	Dymola
1	E_{fd0}	1.327474832534790	1.327474594116211
2	P_{m0}	0.4	0.4
3	I_{D0}	0.2169	0.216949
4	I_{Q0}	0.3404	0.340392
5	Angle	28.85	28.846

From the results we can see that, two software agreed with each other during initialization state. The error were less than the set tolerance. After that, the dynamic simulation was performed, and the results were shown as in Fig. 4.6(a) to 4.8. Beside the quantities at generator and the load bus,the values of the sub-transient flux linkages and transient voltages were recored and compared. It is significantly that the performances of the Modelica models agreed with the PSS/E reference models in high degree.

From the figures we can see that, during steady state, the load consumption are supplied partly by the generator and partly by the infinite bus. When the additional load was added into the system, there occurred a negative mismatch between the mechanical and consumed electrical power which forced the generator to slow down. But since the equivalent impedance at the load bus was reduced, thus the field current of the generator merged instantaneously.

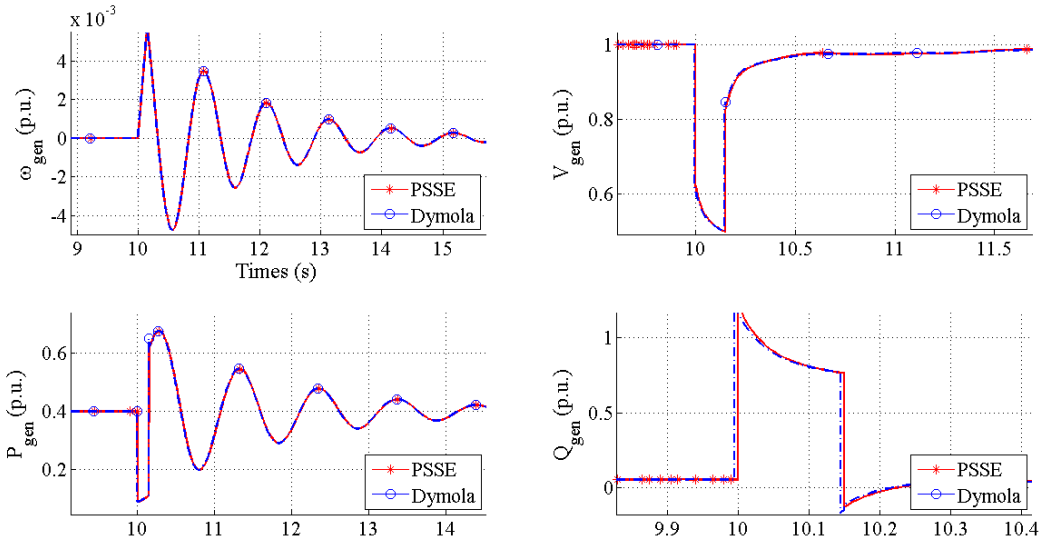

(a) Generator terminal quantities.

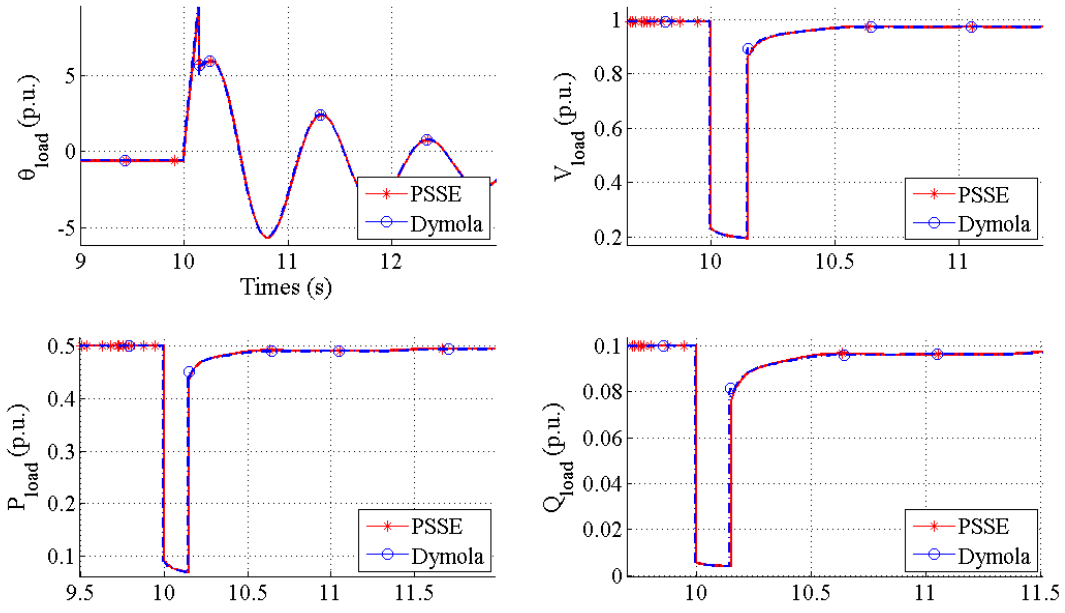

(b) Load bus quantities.

Figure 4.6: GENROU validation results: node bus quantities

As there were neither exciter nor governor equipped in the generator unit, the field voltage and mechanical power remained their initial value during the whole simulation. Due to the infinite inertia of the remote system, the transient of the generator would die out and return to its steady state. Follow the first perturbation, at $10s$ the three phase fault was applied, due to the low impedance of the fault, other electrical components were short circuited which are reflected as magnitude of all bus voltage reduced abruptly. The calculated generator reactive power was higher which attempted to maintain the voltage level of the system.

Since the magnetic fluxes in the air-gap can not change their value instantaneously, the resultant equivalent electrical force remained the same value at the instance when the fault was applied. The short circuit current from the generator flowed through line impedance to the fault. Because of the low impedance of the transmission system, the value of short circuit current was very high compared to normal operation. This is shown in Fig. 4.8, where there existed a surge of generator current directly followed the fault.

The electrical torque kept its pre-disturbance value as well as the power. Due to the low resistance of the post fault system, the delivered active power dropped significantly, hence there exist a unbalance between the generation and consumption. The result was increasing of the generator speed shown in Fig. 4.6(a).

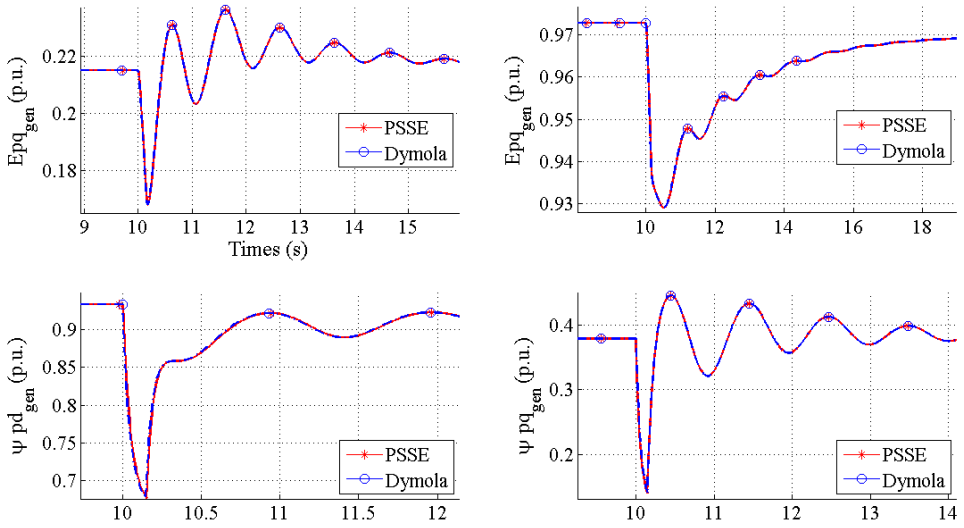

Figure 4.7: GENROU validation results: Generator transient and subtransient electric voltage and flux.

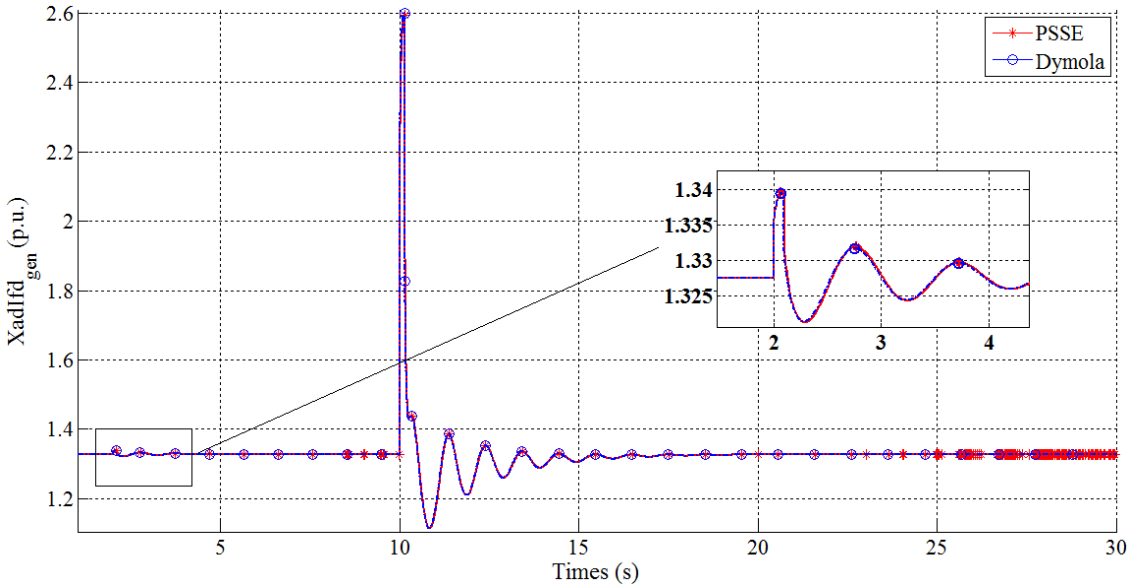

Figure 4.8: GENROU validation results: Generator terminal current.

4.1.2 Validation of Gensal

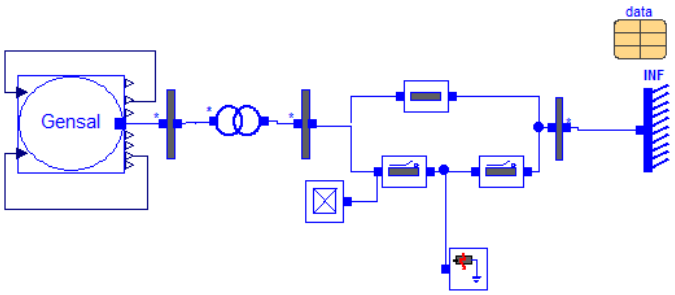

Figure 4.9: Diagram in Dymola of GENSAL test system.

The validation of Gensal model has been proved by the same test system used when testing Genrou. For the sake of saving space the plots were not shown here. The results shown in this section were those from a test system with some modification introduced to the basic scenario. The diagram used in the test system is the one in Figure4.9. The purpose for the modification are that on one hand to confirm the function of bus with changing base, and on the other hand the function of two winding transformer with phase shift. The network data were attached in Appendix. The parameters for generator were entered on machines' base (60 MVA and 1000 MVA) which were different from the power rating of the system (100 MVA). Meanwhile the network were expressed on system base.

When connecting bus with different nameplate voltage, an transformer should be introduced to adjust the voltage. Different connection of the transformer will result in a phase shift between the sending and receiving end bus voltage phasor. There were two transformers equipped in the test system, the upper one connected in a way which will not introduce phase shift, but lower one can result in 30 degree lead at primary side. The impedance and other parameters for the transformers are provided in the Appendix. In order to validate the phase shift function of the transformers, the angle difference between the sending and receiving ends were plotted and compared in Figure4.10(b).

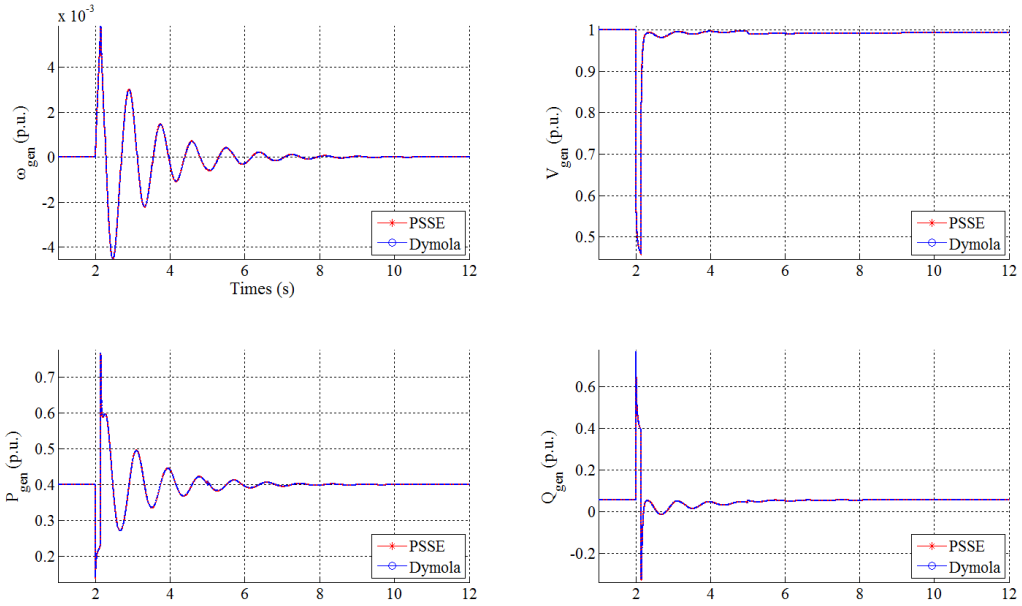

(a) Generator terminal quantities.

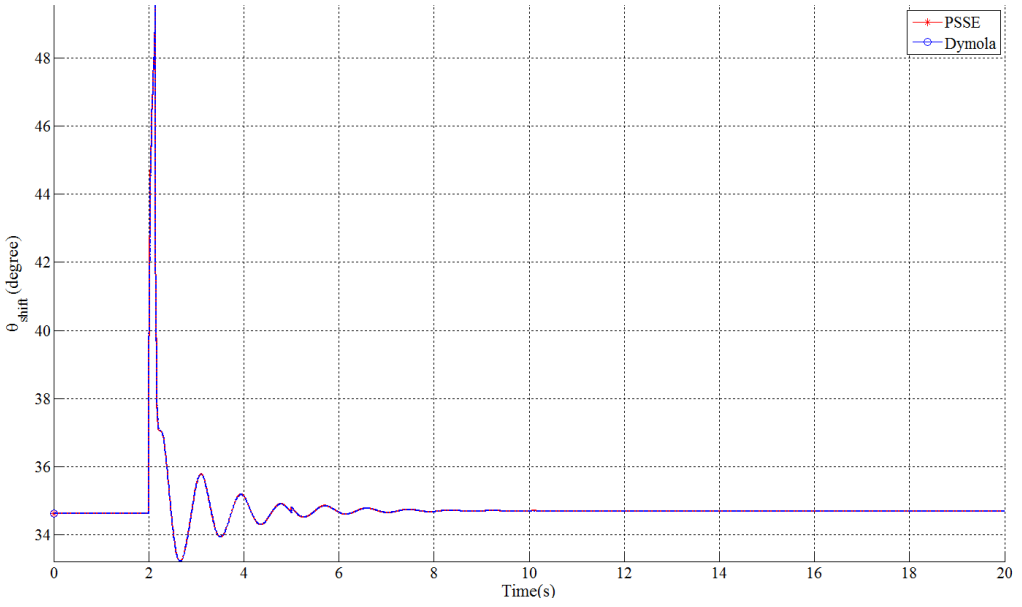

(b) Bus voltage's angle shift between sending and receiving ends of the transformer.

Figure 4.10: GENSAL validation results

Figure 4.10(b) shows us that, the angle shift of transformer from two software matches each other very well. The system in Dymola is identical to the reference PSS/E test system both in initialization and dynamic state. The results proved the behavior of model Gensal and the actions of changing power and voltage base. By including these changing base action, it is possible to use the developed library to present larger system which might include several machines with different power rating connected by step-up or set-down transformers with phase shift. Since the changing base action has been proved, for the sake of convenient, the following test were performed with all parameters on system base.

4.1.3 Validation of IEEET2 and IEESGO

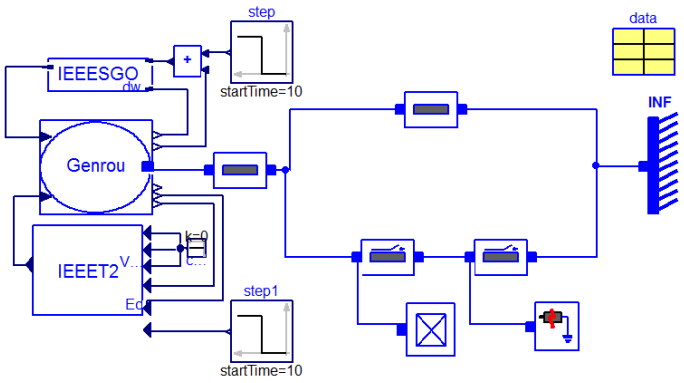

Figure 4.11: Diagram in Dymola of the 3_{rd} test system.

The test system is used to validate the transient response of exciter IEEET2 and governor IEESGO. Below is a list of simulations to be performed and diagram of the test system in Dymola. The results are shown in Figure4.12 to **??**. The three phase to ground fault was applied at same location with the same range as the two previous cases.

The regulators contributed new dynamics to the system and they will be discussed later. After the fault was cleared, the reference step changes were applied. The results shown us that the regulators modeled in Modelica functioned very well since the system behavior in two software confirmed each other. The further comparison are done by plotting the percentage error of the records.

Table 4.10: List of simulations

Step	Scenarios
1.	running under steady state for 2 seconds.
2.	Apply three phase to ground fault as shown in Figure4.2(a).
3.	After $0.15s$ later, the fault was cleared by tripping the line.
4.	Run simulation to $10s$.
5.	Apply $-0.002p.u.$ step in governor reference.
6.	Apply $0.01p.u.$ step in exciter reference.
7.	Run simulation until 20 seconds.

First, the system are compared in general by comparing the generator speed, voltage and power transfer information. There are shown in Fig. 4.12. From the figure, we can see that, with the added control devices, the behavior of the generator in Dymola is matching with that from PSS/E. It indicate that, the system and the applied perturbation are similar.

But in order to validate each control device, the input and output of the device were also compared. The input of the excitation system are the generator terminal voltage while that of the governor system are the speed of the machine. The absolute different of these two variables from two software are plotted. The results were shown in Fig. 4.13.

When the three phase to ground fault was applied, regulators of the generator detected the changes caused by the faults. The increasing of the speed activated the governor system, and the mechanical power was then reduced in order to decrease the accelerate power which can be seen in Fig. 4.14.

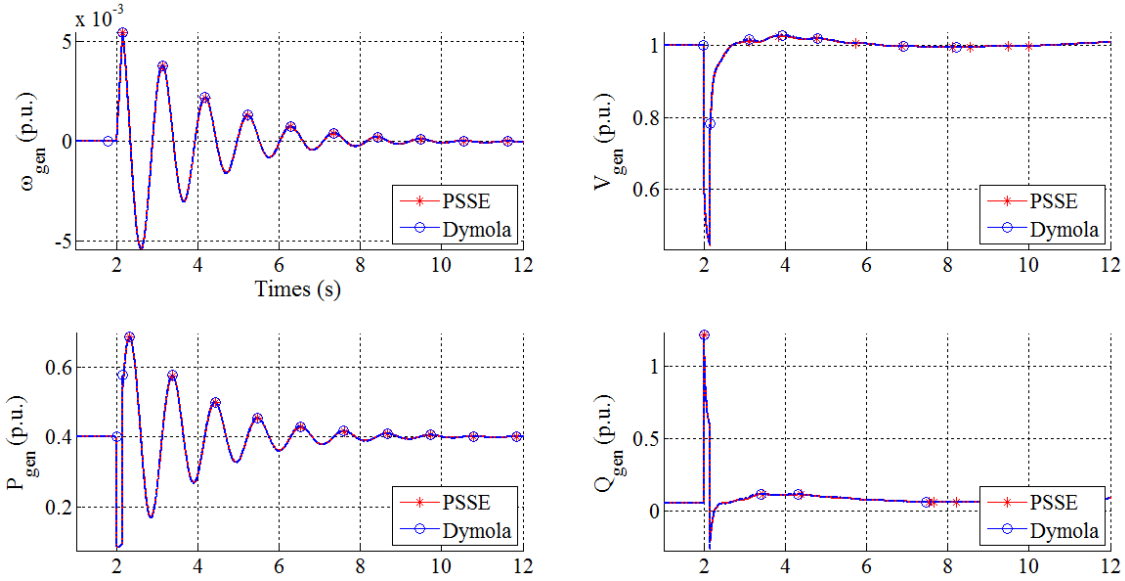

Figure 4.12: Validation result of IEEET2 and IEEESGO test system

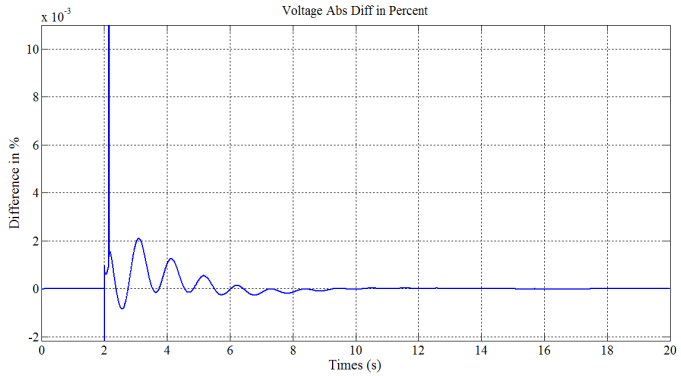

(a) Absolute different of the generator terminal voltage, input of IEEET2:

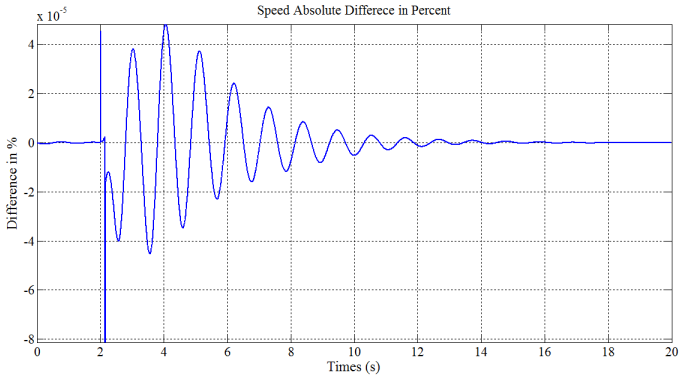

(b) Absolute different of the generator speed input IEEESGO:

Figure 4.13: Validation result of IEEET2 and IEEESGO

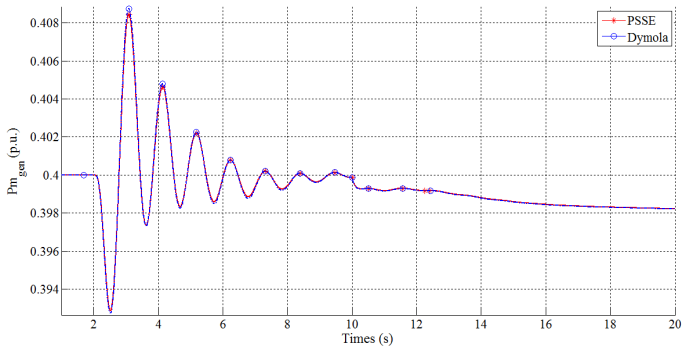

Figure 4.14: Output of IEEESGO: Generator mechanical power

While the drop in generator terminal voltage alarmed the excitation system to increase the field voltage. By doing this the excitation system attempted to increase the induced voltage in the armature windings in order to compensate the big drop. The reaction of exciter was shown in Fig. 4.15(a). However, due to the limit of power supply, the output of the exciter regulator was saturated and remained its upper limit $4p.u.$ during the fault.

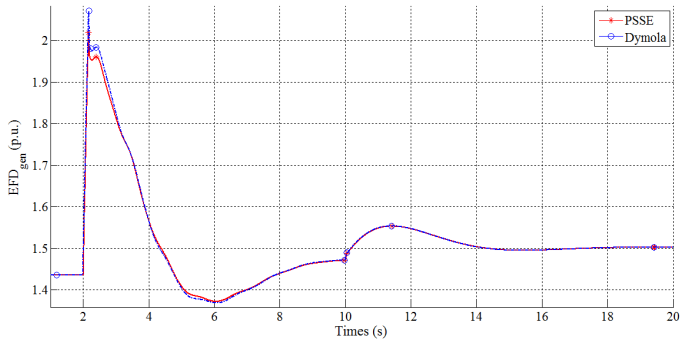

(a) Output of IEEET2: Generator field Voltage

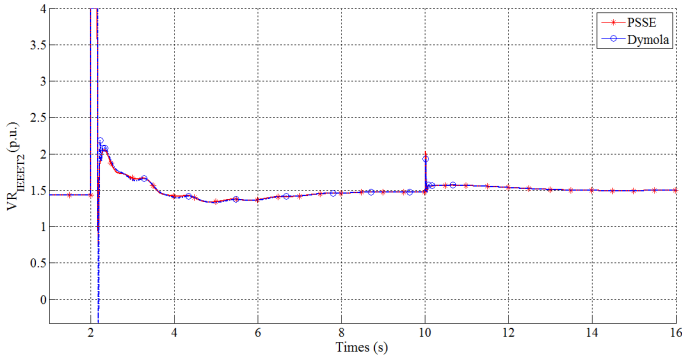

(b) Inner state of IEEET2: Output of voltage regulator

Figure 4.15: Validation result of IEEET2

$0.15s$ later, the fault was clear by tripping the line. The impedance of the network recovered and as a result the current flowed out of the generator drop suddenly. But the value are still higher than its normal operation value because the electric magnetic force were lifted up by the exciter during the fault, and hence still kept its instant value when the fault was cleared. The

active power consumption were then lifted up, remind that at this time the mechanical output from the governor system has been decreased which now resulted in a negative power unbalance. The generator was then slowed down. And following the clearing of the fault, the current fed by the generator reduced thus the system bus voltage recovered. But they were a bit higher than the steady state values. The overshoot of the bus voltage was caused by the regulator system.

As a result of rising swing of the bus voltage, the generator is delivering more power to the system which can be confirmed by the similar overshoot in the plots of power. The generator was then further slow downed. Once again the governor detected the speed deviation, and then raised the mechanical power. The governor attempted to cancel the speed varying of the generator.

The transient of the system had almost died out at around $10s$, the system would return to its steady state if not more perturbation was applied. But at this time, the reference step changes were applied to both governor and exciter. The regulators tried to meet the requirements thus instead of returning to its original equivalent point, the system would finally return to the new stationary state as set by the new reference. The Figures in 4.12 showed that, the final value of generator bus voltage was 0.01 pu higher then the original steady state value. And the mechanical output of the governor is 0.002 lower than the previous equivalent point. The system reacted in the same way before, during, and after all the perturbation, it is fair to conclude that, the Modelica models, IEEET2 and IEESGO have been proved.

4.1.4 Validation of SCRXS and HYGOV

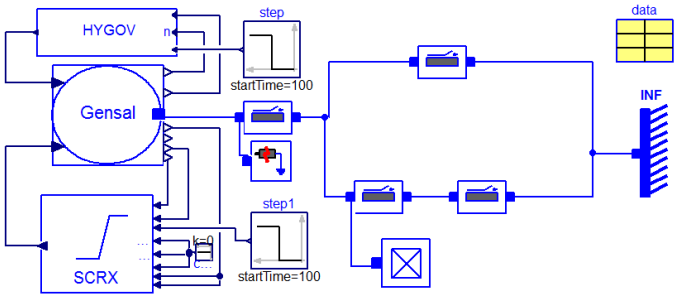

Figure 4.16: Diagram in Dymola of the test system.

The dynamic components in this test are model SCRXS and HYGOV. In order to completely validate the transient behavior of the two models, the simulation scenario was selected as list below. The specific scenario could active the "Negative current logic" inside model SCRXS and made the governor HYGOV hits its no-windup limit. Thus beside the those quantities shown in previous tests the variables such as the water velocity and desired gate position had been plotted as well. Specific attention should be paid to the validation of model SCRXS, since as it would behavior differently according to a zero or no-zero value of the parameter $\frac{r_c}{r_{fd}}$.

Table 4.11: List of simulations

Step	Scenarios
1.	running under steady state for 2 seconds.
2.	Apply three phase fault as shown in Figure4.2(b) with conductance $X = -0.5$.
3.	After $0.15s$ later, the fault was self cleared.
7.	Run simulation until 20 seconds.

To force the generator current to be negative, which means the generator is forced to consumed

reactive power. The perturbation could be a fault which was modeled by connecting an admittance directly to the generator terminal bus. Since the analysis of the fault have been covered in previous example and the focus of this thesis is not the fault analysis, thus from now on for the rest of the tests, only the comparison results will be shown without explanation of the behavior of the variables.

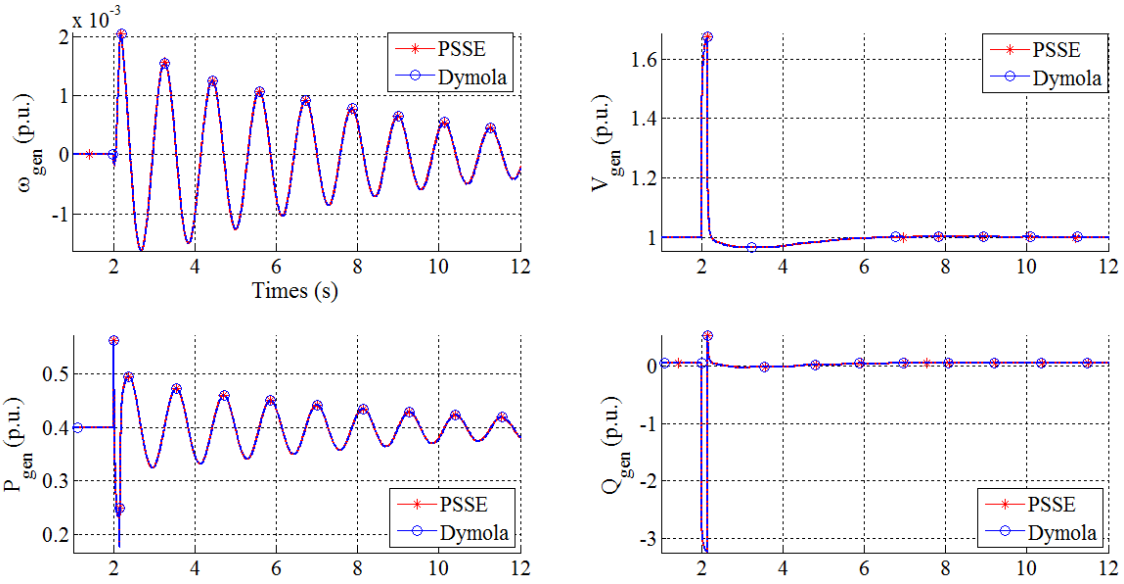

Figure 4.17: Validation result of SCRX and HYGOV test system: Generator quantities

From the figures we can see that once the unbalance between mechanical and electrical power cause the speed to drop. The governor detected the decreasing of the speed then opened the gate immediately. Initially, the power was used to speed up the water at the gate thus there was a some mechanical power drop at the beginning. After that, it is clearly that more mechanical power has been injected into the system. The behavior of the models in two software are similar in high degree thus the model HYGOV can be considered to be validated.

From Fig. 4.17 and 4.19(b), we can see that SCRX detected the high voltage at the terminal of the generator and attempted to lower down the field voltage immediately. However, from Fig. 4.19(a) and 4.19(b) we can see that, the output of SCRX reached the limit of zero once the generator field current went lower than zero. This illustrate that the protect circuit in SCRX was active. If $\frac{r_c}{r_{fd}}$ was set to be 10, then the SCRX responses as shown in Fig. 4.19(d). In the figure we see that, the output of SCRX was proportionally to that of generator field current. All the results from both software matches each other perfectly thus we can concluded that, the model SCRX was validated.

4.1.5 Validation of IEEET1, STAB2A and LFDRAL

The system used to validate components IEEET1, STAB2A and LFDRAL are shown in Fig. 4.20. The generator GENROU was equipped with an excitation system IEEET1 with a stabilizer STAB2A. The load is a frequency dependent composite load. The simulation are listed in Table 4.12. IEEET1 works to keep the voltage of generator bus at desired value by providing suitable field voltage to the generator. STAB2A takes the information of system oscillation by measuring the electric power output of the generator. Base on that, it works to provided compensation signal to IEEET1 in order to wipe out unnecessary oscillation caused by the excitation system.

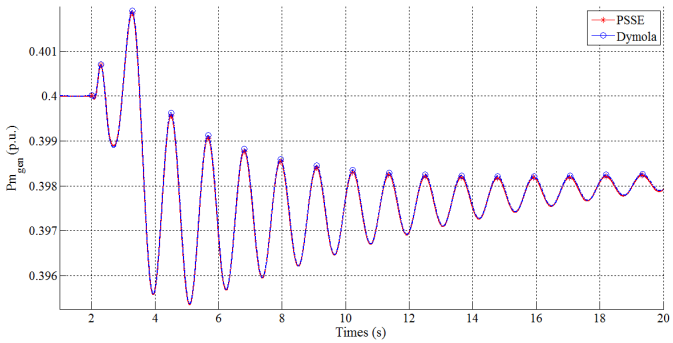

(a) Output of HYGOV: Generator mechanical power

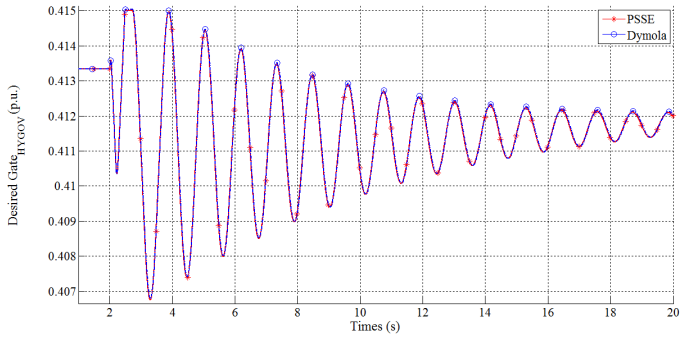

(b) Inner state of HYGOV: Desired gate position

Figure 4.18: Validation result of HYGOV

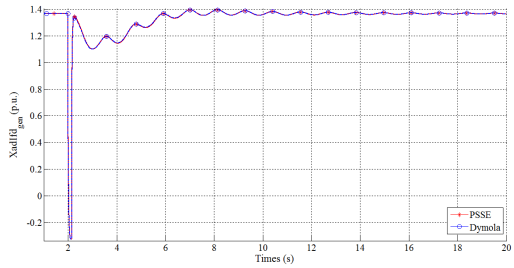

(a) Input of SCRX: Generator field current $\frac{r_c}{r_{fd}} = 0$

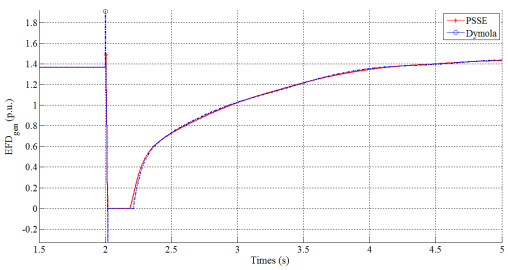

(b) Output of SCRX: Generator field voltage $\frac{r_c}{r_{fd}} = 0$

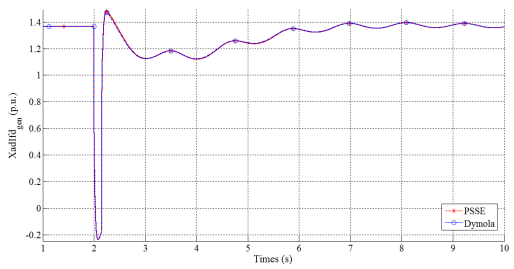

(c) Input of SCRX: Generator field current $\frac{r_c}{r_{fd}} = 10$

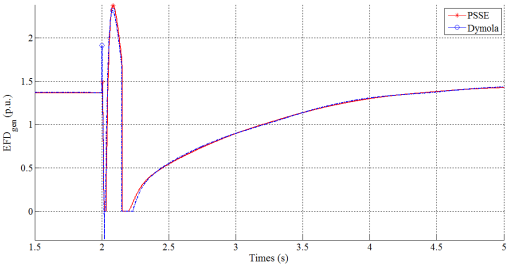

(d) Output of SCRX: Generator field voltage $\frac{r_c}{r_{fd}} = 10$

Figure 4.19: Validation result of SCRX

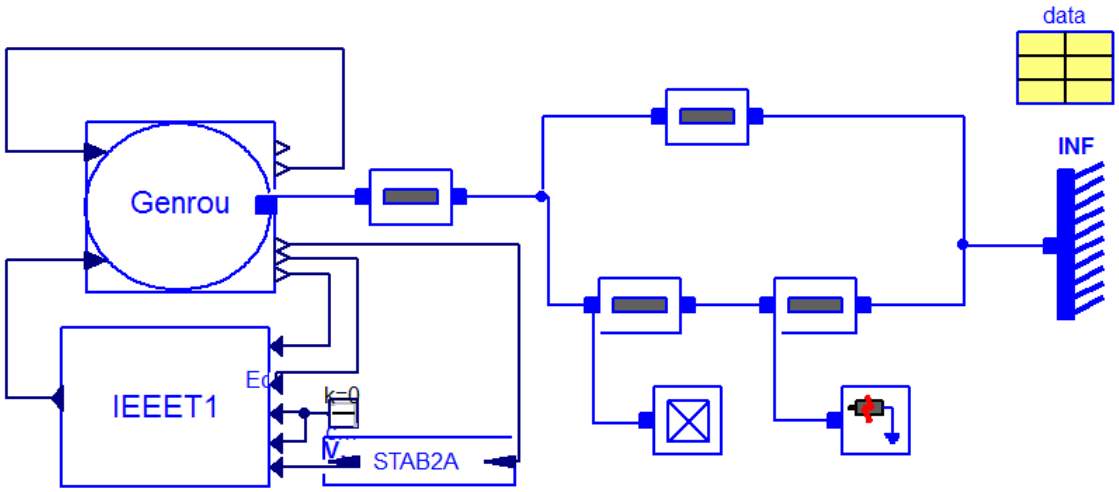

Figure 4.20: Diagram in Dymola of the test system.

In this test, a fault was applied to force the system into transient stage. Besides that, the intensity of the fault was designed to force the model STAB2A to hit its limits. The goal was to see the system behavior when the limitation of the components was hit thus to validate the system as a whole.

Table 4.12: List of simulations

Step	Scenarios
1.	running under steady state for 2 seconds.
2.	Apply three phase to ground fault as shown in Figure4.2(a).
3.	After 0.15s later, the fault was self cleared.
4.	Run simulation until 20 seconds.

From the figure above we can see that the three phase to ground fault caused the voltage at the terminal bus of the generator to drop severely. Thus IEEET1 reacted immediately by raising up the field voltage by which it attempted to level up the dropping bus voltage which was shown in Fig. 4.22(a). Figure 4.22(b) shows us that STAB2A detected the change of electric power from the generator and took action to rise the its output. However, the limitation was hit and insufficient compensation failed to damp out effect of the fault, the system remained oscillating. Thus it is fair enough to conclude that these two components was validated.

In order to validate the component LFDRAL, the quantities at load bus was plotted and compared. The following figures show that the results from two software match with each other perfectly thus we can conclude that LFDRAL was validated.

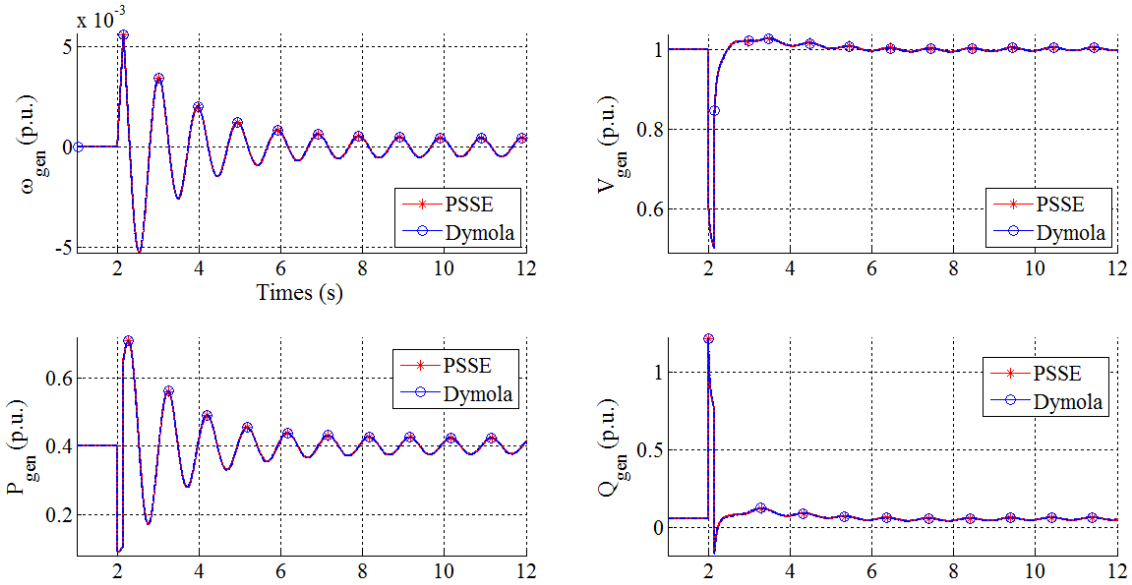

Figure 4.21: Validation result of IEEET1, STAB2A and LFDRAL test system: Generator quantities

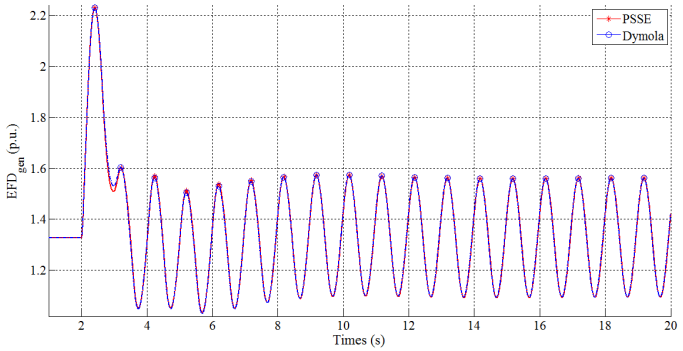

(a) Output of IEEET1: Generator field voltage

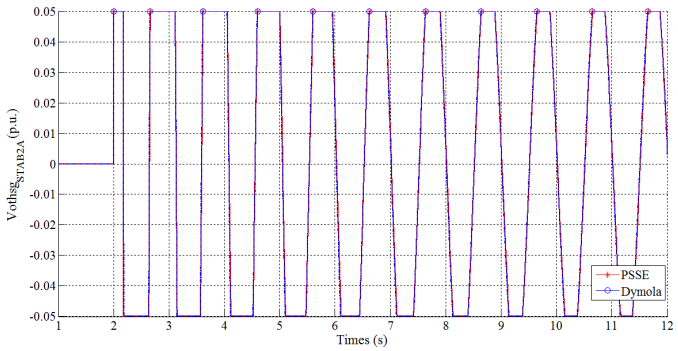

(b) Output of STAB2A: Vothsg

Figure 4.22: Validation result of IEEET1 and STAB2A

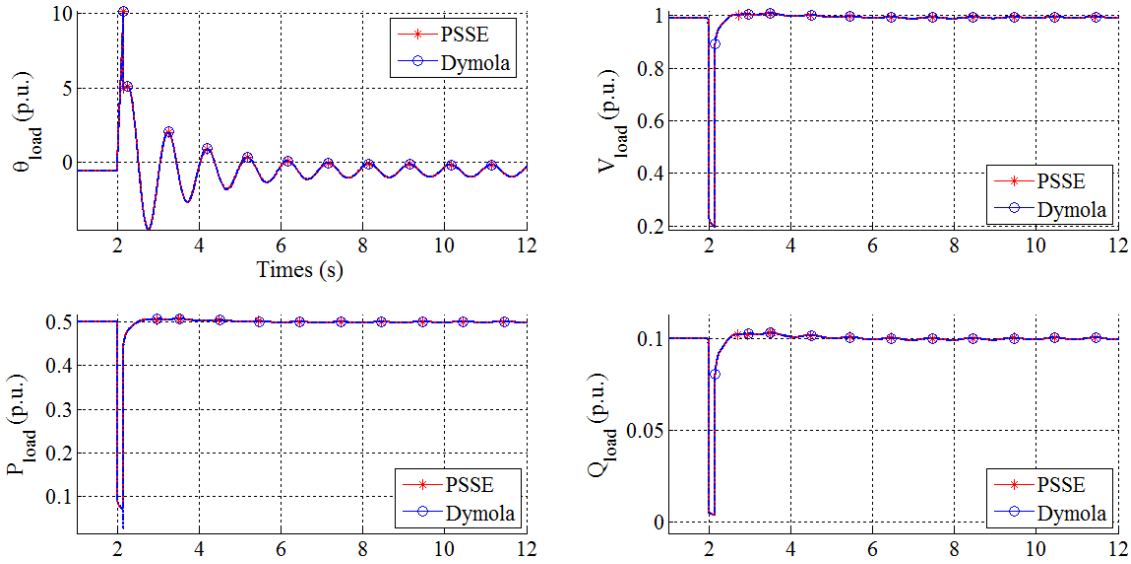

(a) Load bus quantities

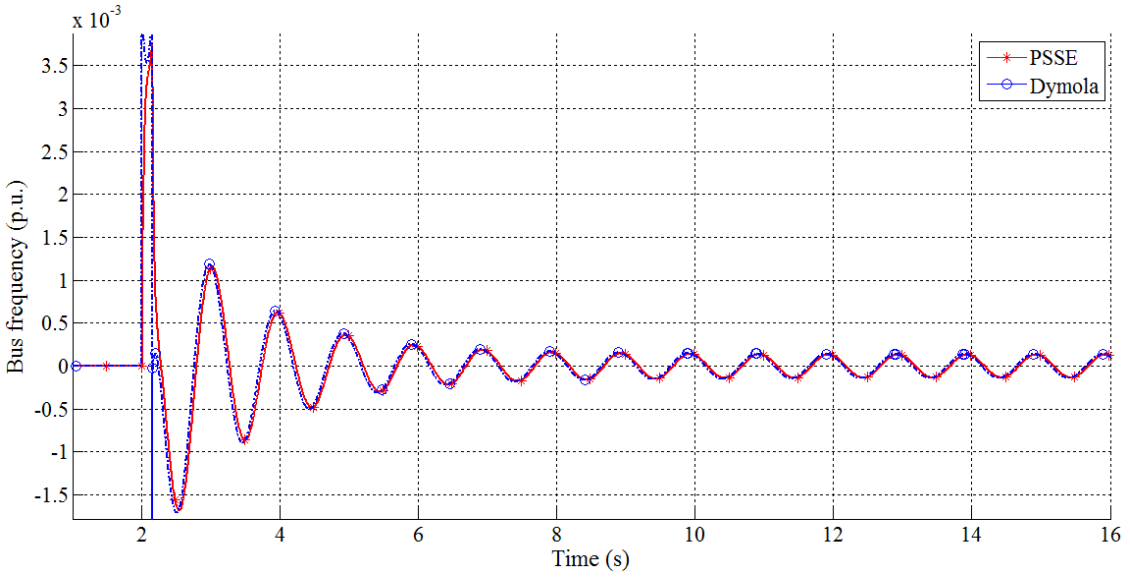

(b) Bus frequency

Figure 4.23: Validation result of LFDRAL

4.1.6 Validation of OLTC

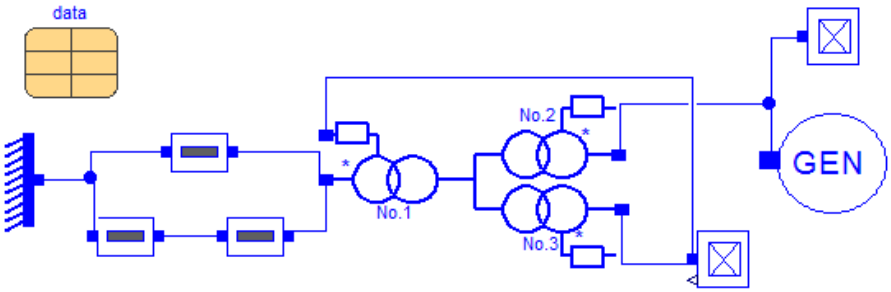

Figure 4.24: Diagram in Dymola of the 5_{th} test system.

The test system used to validate OLTC are shown in Fig. 4.24 and the parameters are given in Appendix. The system model presented that there are three areas connected through a three-winding transformer. The remote power plan was modeled by a infinite bus. The local power plan is modeled by a generator unit which was a GENROU model equipped with IEEET1 and STAB2A. There are mainly consumption in the third zone thus it was modeled by a composite load.

The remote and the local were connected by a three-winding transformer where the infinite bus was connected to the primary side of the transformer, the local unit was to the secondary side of a three winding and a composite load was connected to the tertiary side of the transformer.

The power consumption at zone third was supported by the remote and local power plan together. The voltage at tertiary winding of the transformer is controlled by the OLTC model at primary side. In order to validate the performance of OLTC, the list of simulation were conducted. During the test, the reactive power load were stepped artificially in order to force the OLTC to react.

Table 4.13: List of simulations

Step	Scenarios
1.	Running under steady state for 20 seconds.
2.	Increasing the Q load to 1.5 p.u. in PSS/E it means to add Q load approximately by 1.42 p.u. in Dymola
3.	Simulating to 40 seconds.
4.	Increasing the Q load to 2.2 p.u. in PSS/E it means to add Q load approximately by 0.85 p.u. in Dymola
5.	Simulating to 80 seconds.
6.	Increasing the Q load to 2.5 p.u. in PSS/E it means to add Q load approximately by 0.7 p.u. in Dymola
5.	Simulating to 200 seconds.

There are three stage in total, and the validation results are shown here. From the following figures we can see that, after the first step of the Q load, the tertiary side voltage dropped out of the control band at first but recovered to stay in the control band in a short time. The time period was less then the control delay thus OLTC didn't react.

The second stepping-up of the Q load force the voltage to drop further, and this time it didn't manage to go back to the control band thus after delay for $T_C = 17s$, OLTC took action to increase the tap ratio thus the voltage at the primary side was stepped down while the voltage on

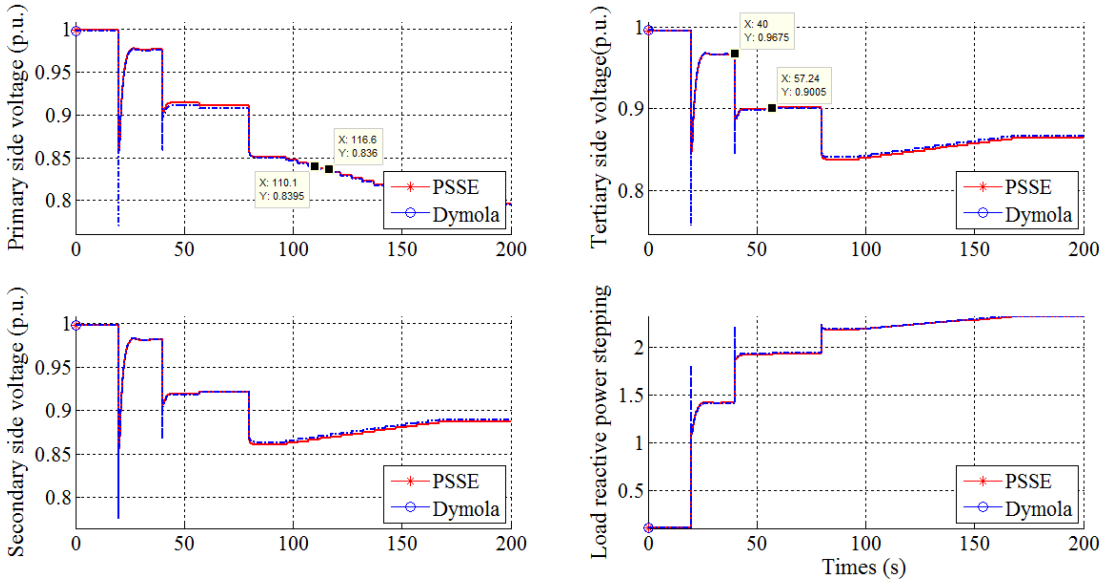

Figure 4.25: Validation results of OLTC

the secondary side was stepped up.

The third stepping-up of the Q load cause the voltage to drop so sever thus the OLTC hit its limits and failed to bring the voltage back to the control band. From the figure we can see clearly that, there was a $T_D = 5s$ delay for OLTC to perform a tap change. Beside that, we can see that, there were 16 steps in total before OLTC hit its limits. Thus it proved that, the OLTC model in Dymola applied the desired delay during changing the tap ratio and the tap was put at the middle of the total 33 step position. From these test results, we can conclude that, the model was validated successfully.

4.2 Real World Power System

4.2.1 AKD

System model AKD is a subset model of Norwegian grid. The system setup is shown in Fig.4.26. It contains five detail generator models All of them are Model Gensal. The three generators on the upper side are the equivalent models of remote grid and the rest two generators which are connected to the network through transformers are the equivalent models of the local grid. These two generators are equipped with regulators. They are governor HYGOV, exciter IEEET2, and stabilizer IEEEST.

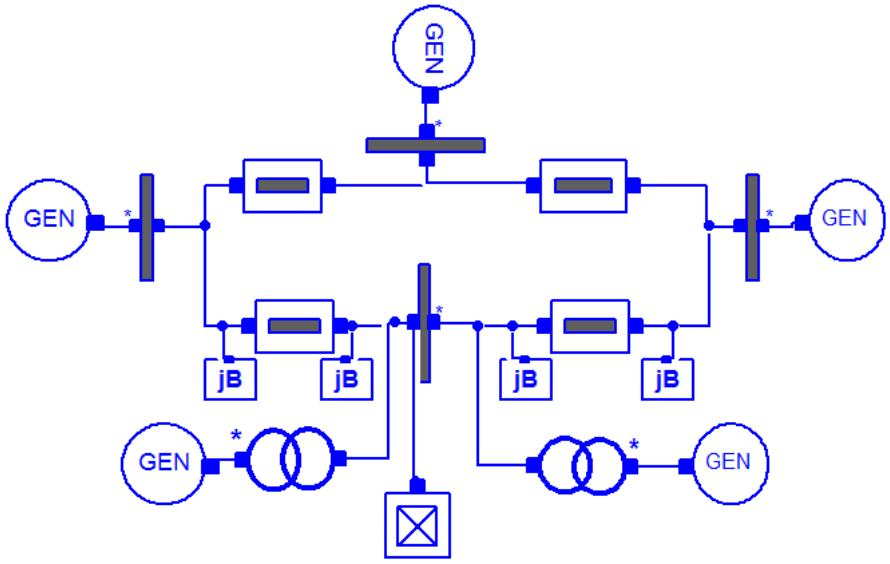

Figure 4.26: Test system diagram

The performed simulations are listed here. Since all of the components have been validated through the small scale systems in previous section, the goal of the test here is only to check the simulation results of the system with more complex structure. From the test system diagram we can see that, there is a power flow loop and there are two transformer are introducing phase shift. This structure increase the complexity of the calculation.

Table 4.14: List of simulations

Step	Scenarios
1.	Running under steady state for 1s.
1.	Open the line for 0.15s.
1.	Apply 3phtgf at 7.5s; 0.15s later, clear the fault.
1.	Run simulation until steady state.

However, the simulation results in the following figures show that, the Modelica model can represent the similar dynamic of the reference PSS/E model. There are not problem for Dymola to perform the simulation for this system model. Thus it is fair to say that now, the models can replace the original PSS/E model when performing analysis of Norwegian power grid.

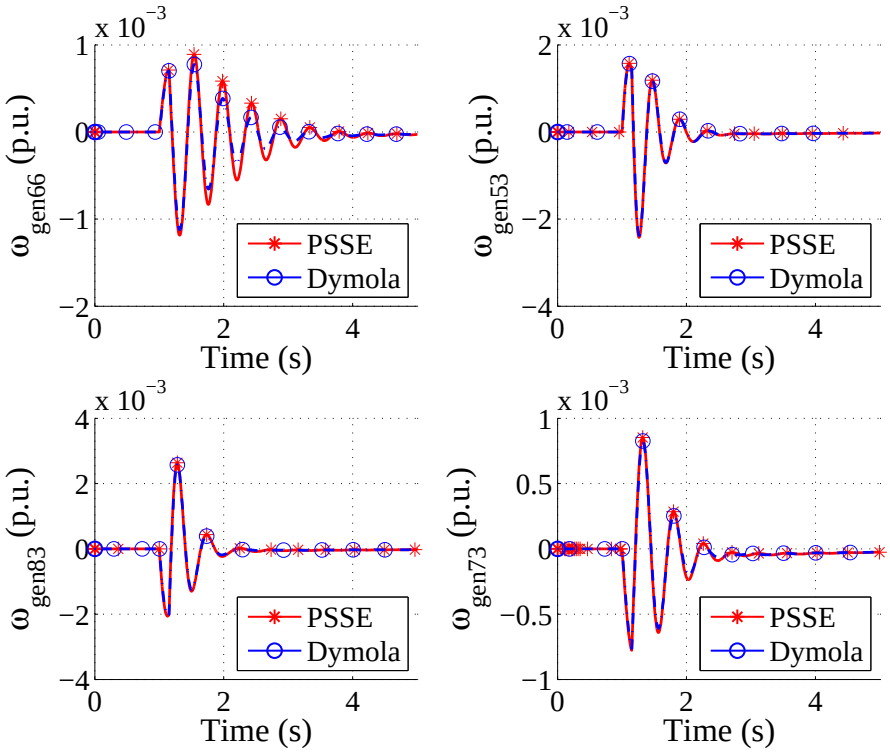

(a) Generator speed variation(1).

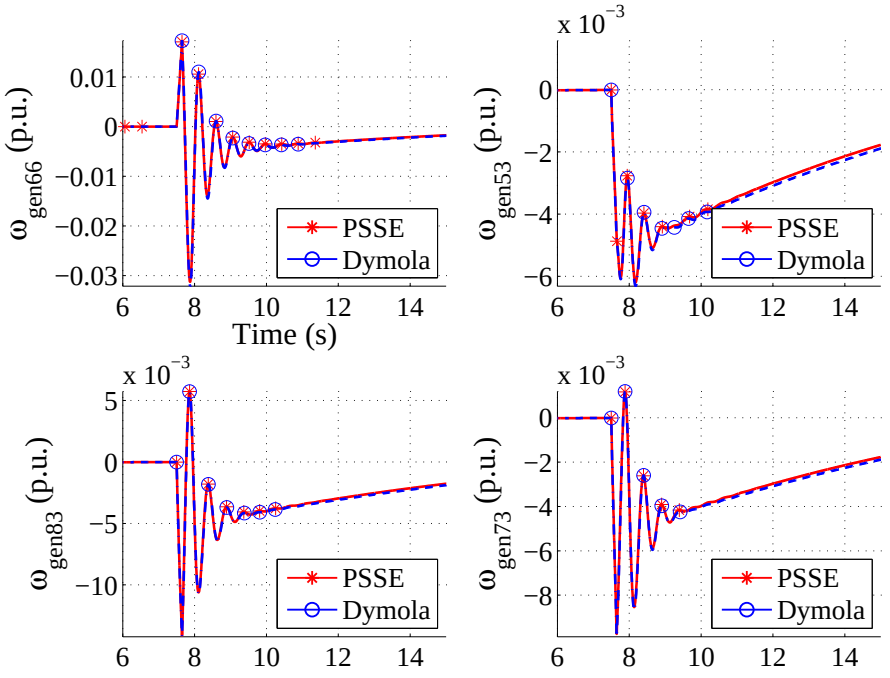

(b) Generator speed variation(2).

Figure 4.27: Validation result of AKD test system(1).

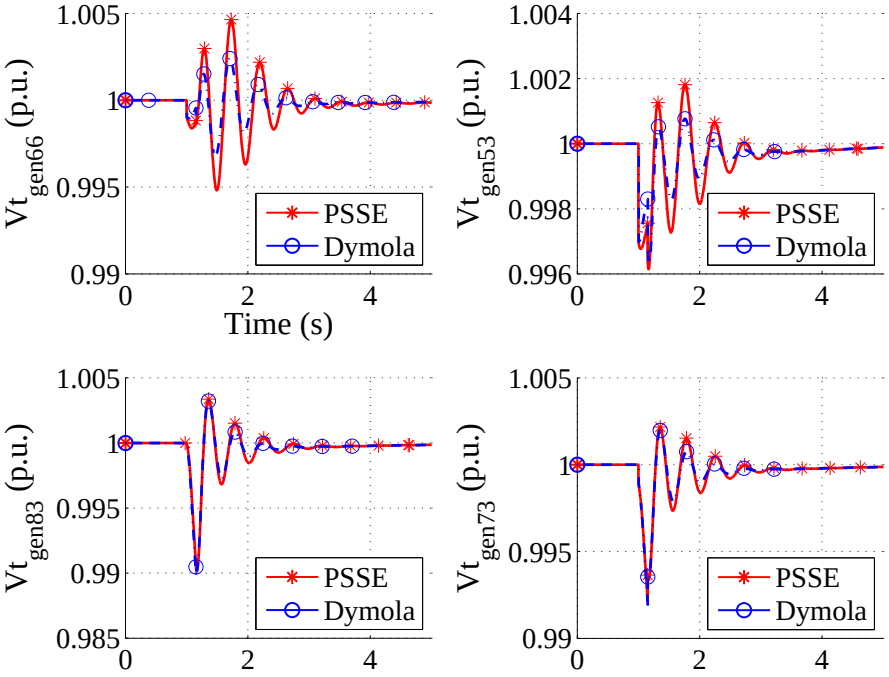

(a) Generator bus voltage (1).

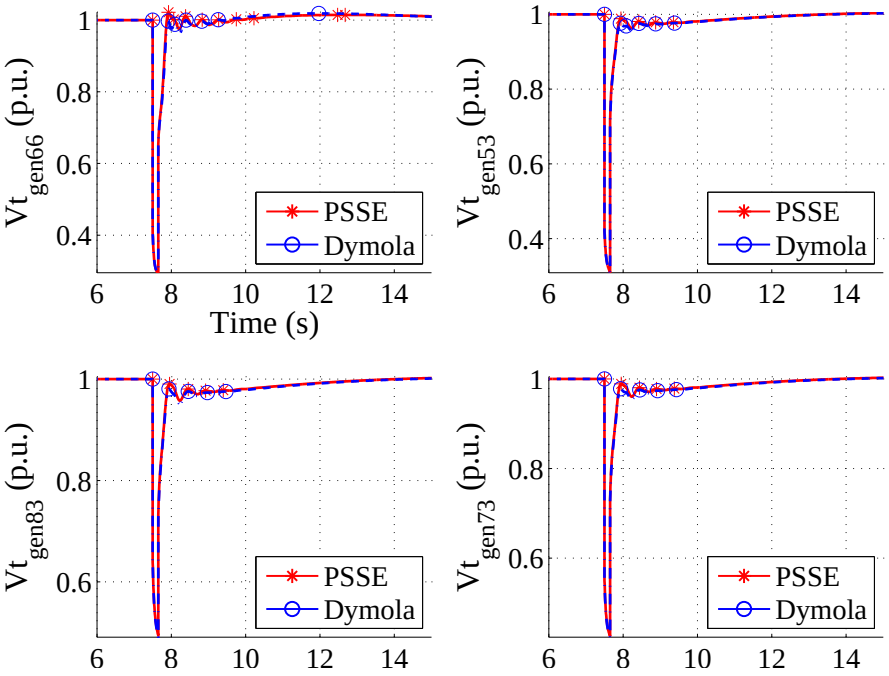

(b) Generator bus voltage (2).

Figure 4.28: Validation result of AKD test system(1).

5 Conclusion

In this project, the main objective was to develop and validate Modelica models for each of the grid components included in a predetermined list of subset of the Norwegian grid. The work has been carried out in several steps, with first a study of the reference models in PSS/E, the implementation in the Modelica languages and finally the validation by comparing dynamic simulations between the reference platform (PSS/E) and Modelica.

All simulation show results with a high degree of similarity between the dynamic behavior of the developed models and the reference model. The main objective of the project is thus achieved successfully

In chapter one, a brief introduction about the background of this project and the motivation to use Modelica in power system analysis has been discussed. In chapter two, the difference between two software Dymola and PSS/E has been studied. It can serve as a reference for one who intend to carry out similar project or to work with these two software.

The modeling method for each components model has been explained in detail in chapter three. For those models which was explained vaguely in PSS/E documents, revisions have been carried out and the performance of them have been proved by validation tests. Thus I can conclude that, the models are now ready to be used in iTesla project. And all future user can have the access to both the source code and modeling methods of the models. This will facilitate the reuse of the models. The models can be utilized in all software which can support Modelica language. Furthermore, the models can be simulated in Matlab through Function Mock Unit (FIM) tool box.

All of the data file concerning the validation tests have been documented properly which can be sued to check the work of the project. The procedures of performing validation tests have been explained step by step in previous chapter. Thus it is easy for one to follow up the work if there is any need to carry out more tests.

Finally, for those who are working with building Modelica models, the Some suggestion towards debugging procedures have been summarized as following. Basically, to ask the following questions can help one debug the models efficiently.

1. Has the model been initialized correctly ?

   For example, if the records of one variable from PSS/E and Dymola starts from the same points which means the power flow records are entered correctly. Further more, if the results agree with each other during a few second before applying the faults. It means the model is initialized correctly. It is better to make sure that the initialization are correct and then go further to dynamic simulation.

2. Are the applied faults in both systems the same or not ?

It is easier to check the perturbation cases before going through the equations of the models. For example, during load variation, there are several options available in PSS/E, the one with varying the load with constant P Q ratio was applied in the tests. Also, there are some trivial issues might introduce the differences, like the load will be shed down by a factor when the bus voltage goes lower then 0.8 p.u.. To reach good similarity, this particular assumption should also be implement during tests.

3. Is there anything wrong in the model expression (equations or parameters) ?

   Typically, the problems can be caused by the parameters or mathematic equations. If the records show the same tendency but difference in magnitude or frequency then most of time it is caused by typing the wrong parameters. On the other hand, if the tendency is not the same, then some of mathematic equations must be wrong. they could either be typed wrongly, or be implemented in a way where Modelica has different interpretation of them. The suggestions are that to study the equations carefully, highlight the suspected ones, and test them separately.

4. Are the set up of two systems are identical or not ?

   The solution results from different solvers might show different inertia. That's why we said it is better to start with the same solvers. One the other hand, attentions should be paid to the plot interval and the time step if a fix step solver is applied, because the model could behavior wrongly when too large time step is applied.

A Appendix

A.1 Dynamic parameter

Listing A.1: Dynamica parameters of Genrou test

```
1       1 'GENROU' 1     5.0000       0.50000E-01  0.70000       0.10000
2           4.0000       0.0000        1.4100       1.3500       0.30000
3          0.60000      0.20000       0.12000      0.10000       0.50000/
4       3 'GENCLS' 1     0.0000        0.0000/
```

Listing A.2: Dynamica parameters of GENROU+IEEET2+IEESGO test

```
1       1 'GENROU' 1     5.0000       0.70000E-01  0.90000       0.90000E-01
2           4.2800       0.0000        1.8400       1.7500       0.41000
3          0.60000      0.2000       0.12000      0.11000      0.39000 /
4       1 'IEEET2' 1     0.0000        100.00      0.14000E-01    4.0000
5          -4.0000       1.0000       0.62000      0.12000       1.0000
6          0.10000       2.3100       0.80000E-01   3.0800       0.30000/
7       1 'IEESGO' 1    0.20000        0.0000      0.50000       0.12000
8           5.0000      0.50000        20.000      0.59000       0.43000
9          0.98000       0.0000    /
10      3 'GENCLS' 1     0.0000        0.0000    /
```

Listing A.3: Dynamica parameters of GENROU+STAB2A+IEEET1+LDFRAL test

```
1         1 'GENROU' 1     5.0000       0.50000E-01  0.70000       0.10000
2             4.0000       0.0000        1.4100       1.3500       0.30000
3            0.60000      0.20000       0.12000      0.10000       0.50000/
4         1 'STAB2A' 1     1.0000        4.4000       10.000        1.8000
5             1.0000       1.4100       0.10000E-01  0.50000E-01/
6         1 'IEEET1' 1     0.0000        50.000      0.50000        3.0000
7            -3.0000       0.0000       0.80000      0.78000E-01  0.72600
8             0.0000       2.4000       0.30000E-01   5.0000       0.50000/
9         3 'GENCLS' 1     0.0000        0.0000    /
```

Listing A.4: Dynamica parameters of GENSAL+IEEEST+SEXS test

```
1         1 'GENSAL' 1     6.7000       0.28000E-01  0.35000E-01   4.4100
2             0.0000       1.2200       0.76000      0.29700       0.24000
3             0.12200      0.18600      0.80200    /
4         1 'IEEEST' 1       1           0          0.0000      0.0000
5              0.0000       0.0000       0.0000      0.0000     0.1535
6              0.05060      0.8971          1           1.5        1.5
7               15           0.1         -0.0500      0.0000      0.00000/
```

```
8         1 'SEXS'   1      0.10000        10.000    100.00      0.0200
9             0.0000        4.7300     /
10        3 'GENCLS' 1      0.0000     0.0000     /
```

Listing A.5: Dynamica parameters of GENSAL+SCRX+HYGOV test (rcrfd 0)

```
1         1 'GENSAL' 1      6.7000       0.28000E-01  0.35000E-01    4.4100
2             0.0000        1.2200       0.76000      0.29700       0.20000
3            0.12000       0.18600       0.80200     /
4         1 'SCRX'   1      0.10000        10.000        100.00       0.50000E-01
5             0.0000        5.0000        0.0000        0.0000     /
6         1 'HYGOV'  1     0.50000E-01   0.30000        5.0000       0.50000E-01
7            0.50000       0.20000E-01   0.41500        0.0000        1.2500
8             1.2000       0.20000       0.80000E-01/
9         3 'GENCLS' 1      0.0000        0.0000     /
```

Listing A.6: Dynamica parameters of GENSAL+SCRX+HYGOV test (rcrfd 10)

```
1       1 'GENSAL' 1      6.7000       0.28000E-01  0.35000E-01    4.4100
2           0.0000        1.2200       0.76000      0.29700       0.20000
3          0.12000       0.18600       0.80200     /
4       1 'SCRX'   1      0.10000        10.000        100.00       0.50000E-01
5           0.0000        5.0000        0.0000        10.000     /
6       1 'HYGOV'  1     0.50000E-01   0.30000        5.0000       0.50000E-01
7          0.50000       0.20000E-01   0.41500        0.0000        1.2500
8           1.2000       0.20000       0.80000E-01/
9       3 'GENCLS' 1      0.0000        0.0000     /
```

Listing A.7: Dynamica parameters of GENSAL test

```
1       1 'GENSAL' 1      5.0000       0.50000E-01  0.10000       4.0000
2          0.0000       1.4100        1.3500       0.30000       0.20000
3          0.12000       0.10000       0.50000/
4       3 'GENCLS' 1      0.0000        0.0000/
```

Listing A.8: Dynamica parameters of test including three windings transformer

```
1       3 'GENCLS' 1      0.0000        0.0000/
2     102 'GENROU' 1      5.0000       0.50000E-01  0.70000       0.10000
3           4.0000        0.0000        1.4100        1.3500       0.30000
4          0.60000       0.20000       0.12000       0.10000       0.50000/
5     102 'STAB2A' 1      1.0000        4.4000        10.000        1.8000
6           1.0000        1.4100       0.10000E-01  0.50000E-01/
7     102 'IEEET1' 1      0.0000        126.00       0.50000        3.0000
8          -3.0000        0.0000       0.80000      0.78000E-01  0.72600
9           0.0000        2.4000       0.30000E-01   5.0000       0.50000/
```

References

[1] iTesla,url=http://www.itesla-project.eu/.

[2] Modelica,url=https://www.modelica.org.

[3] Dymola, Dynasim,url=www.dynasim.se.

[4] Dymola Manual Version 5.3a, Dynamic Modeling Laboratory, Dynasim AB, Sweden.

[5] Panciatici, P.; Chieh, AS., "Equation-based hybrid modeling of power systems for time-domain simulation," Power and Energy Society General Meeting, 2011 IEEE , vol., no., pp.1,9, 24-29 July 2011. doi: 10.1109/PES.2011.6039155

[6] P.Kundur,*Power System Stability and Control*, McGraw-Hill, 1993.

[7] Federico Milano, *Power System Modelling and Scripting*, Springer, 2010.

[8] IEEE Standard Board, "IEEE Guide for Synchronous Generator Modeling Practices in Stability Analyses", *IEEE Inc* 1991.

[9] Siemens PTI, "PSSE Program Application Guide v.30.2",Siemens Power Transmission & Distribution Inc.,Power Technologies International, 2005.

[10] Siemens PTI, "PSSE Program Operation Manual v.30.2",Siemens Power Transmission & Distribution Inc.,Power Technologies International, 2005.

[11] Siemens PTI, "PSSE User Manual v.30.2",Siemens Power Transmission & Distribution Inc.,Power Technologies International, 2005.

[12] Fritzson, Peter. "Principles of object-oriented modeling and simulation with Modelica 2.1," John Wiley & Sons, 2010.

[13] Modelica Association,"Modelica® - A Unified Object-Oriented Language for Physical Systems Modeling,Version 3.2,March 24, 2010.

[14] Panciatici, P.; Chieh, A.S., "Equation-based hybrid modeling of power systems for time-domain simulation," *Power and Energy Society General Meeting*, *IEEE* , vol., no., pp.1,9, 24-29 July 2011 doi: 10.1109/PES.2011.6039155

[15] Chieh, A.S., Panciatici, P., Picard, J., "Power system modeling in Modelica for time-domain simulation,"*PowerTech,2011 IEEE Trondheim*, vol., no., pp.1,8, 19-23 June 2011.

[16] Vanfretti, L., Li, W., Bogodorova, T., "Panciatici, P., unambiguous power system dynamic modeling and simulation using modelica tools," *Power and Energy Society General Meeting (PES)*, *2013 IEEE*, pp.1,5, 21-25 July 2013.

[17] Richard P.Schulz, "Synchronous Machine Modeling", General Electric Company, Schenectady, N.Y. *IEEE* 1975.

[18] IEEE Standard Board, "IEEE Guide for Synchronous Generator Modeling Practices in Stability Analyses", *IEEE Inc* 1991.

[19] IEEE African, "Assessment of Commercially Available Software Tools for Transient Stability : Experience Gained in an Academic Environment", *IEEE Inc*, 2004.

[20] "IEEE Recommended Practice for Excitation System Models for Power System Stability Studies," IEEE Std 421.5-2005(Revision of IEEE Std 421.5-1992) , vol., no., pp.0 1,85, 2006, doi=10.1109/IEEESTD.2006.99499.

[21] Klempner, G. and Kerszenbaum, I.,"Operation and Maintenance of Large Turbo-Generators",*IEEE Press Series on Power Engineering*,Wiley,2004, url=http://books.google.se/books?id=DPdkLp_crLAC

[22] Carlos Grande-Moran,"Modeling of Three-Winding Voltage Regulating Transformers for Positive Sequence Load Flow Analysis in PSS®E",*Siemens Energy, Inc.*,no.106,pp.1-11,July 2010.

[23] Milano, F., "Hybrid Control Model of Under Load Tap Changers," *Power Delivery, IEEE Transactions on*, vol.26, no.4, pp.2837,2844, Oct. 2011.doi=10.1109/TPWRD.2011.2167521 .

[24] Calovic, M.S., "Modeling and Analysis of Under-Load Tap-Changing Transformer Control Systems," *Power Apparatus and Systems, IEEE Transactions on*, vol.PAS-103, no.7, pp.1909,1915, July 1984, doi=10.1109/TPAS.1984.318657.

[25] Turbine & Turbine Governor modeling, Istanbul, May 2011, url=http://64.190.51.133/Programs/Blacksea/Dynamic.

[26] IEEE Committee Report."Dynamic Models for Steam and Hydro Turbines in Power System Studies", *IEEE Trans.*, Vol. PAS-92. pp. 1904-1905, November/ December 1973.

[27] IEEE Working Group Report. "Hydraulic Turbine and Turbine Control Models for System Dynamic Studies ", *IEEE Trans.*, Vol. PWRS-7, No.1, pp.167-179, February 1992.